HHS Public Access

Author manuscript

J Immunol. Author manuscript; available in PMC 2024 August 01.

Published in final edited form as:

J Immunol. 2023 August 01; 211(3): 474–485. doi:10.4049/jimmunol.2200420.

Role of IL-27 in herpes simplex virus-1- induced herpetic stromal keratitis

Ferrin Antony[1], **Chetan Pundkar**[1], **Maninder Sandey**[1], **Amarjit Mishra**[1], **Amol Suryawanshi**[1,*]

[1]Department of Pathobiology, College of Veterinary Medicine, Auburn University, AL, 36849, USA.

Abstract

Herpetic stromal keratitis (HSK) is a painful and vision-impairing disease caused by recurrent Herpes Simplex virus (HSV)-1 infection of the cornea. The virus replication in the corneal epithelium and associated inflammation play a dominant role in HSK progression. Current HSK treatments targeting inflammation or virus replication are partially effective, promote HSV-1 latency, and long-term use can cause undesirable side effects. Thus, understanding molecular and cellular events that control HSV-1 replication and inflammation is crucial for developing novel HSK therapies. In this study, we report that ocular HSV-1 infection induces the expression of IL-27, a pleiotropic immunoregulatory cytokine. Our data indicate that HSV-1 infection stimulates IL-27 production by macrophages. Using primary corneal HSV-1 infection mouse model and IL-27 receptor knockout mice (IL-27R$\alpha^{-/-}$), we show that IL-27 plays a critical role in controlling HSV-1 shedding from the cornea, the optimum induction of effector $CD4^+$ T cell responses, and limiting HSK progression. Using *in vitro* bone marrow-derived macrophages (BMDMs), we show that IL-27 plays anti-viral role by regulating macrophage-mediated HSV-1 killing, IFN-β production, and IFN-stimulated genes (ISGs) expression after HSV-1 infection. Further, we report that IL-27 is critical for macrophage survival, antigen (Ag) uptake, and the expression of co-stimulatory molecules involved in the optimum induction of effector T cell responses. Our results indicate that IL-27 promotes endogenous anti-viral and anti-inflammatory responses and represents a promising target for suppressing HSK progression.

Introduction

HSV-1 is a highly successful pathogen that undergoes life-long latency in the trigeminal ganglion (1–5). Recurrent HSV-1 infection of the cornea causes a severe immuno-inflammatory condition leading to HSK (6). HSK is a painful condition and the leading cause of infectious blindness in the US (3, 7, 8). Globally, 1.5 million cases of ocular HSV-1 infection are reported annually, with 40,000 new cases of severe vision impairment and blindness (3, 7, 8). If left untreated, HSK deteriorates to necrotizing keratitis with a significantly increased risk of corneal melting and perforation (9, 10). HSK lesions in humans are considered an immunopathological consequence of virus replication in the corneal epithelium, followed by activation of host's innate and adaptive immune

*Corresponding author: Phone: 344-844-5580; Fax: (334) 844-2652; amol.suryawanshi@auburn.edu.

responses (6). Accordingly, current HSK therapies are targeted to inhibit virus replication (anti-virals) and suppress inflammation (corticosteroids) (10–13). However, the long-term use of corticosteroids and anti-virals is associated with many side effects such as corneal toxicity, glaucoma, cataract, delayed wound healing, corneal thinning, secondary opportunistic infections, and recurrent episodes of HSV-1 infection (4, 11, 12, 14). Thus, a significant focus of HSK research is to identify the molecular and cellular mechanisms that can simultaneously promote endogenous anti-viral and anti-inflammatory responses after recurrent corneal HSV-1 infection.

Past studies using a murine model of primary and recurrent HSV-1 infection suggest HSK as an immunopathological disease resulting from uncontrolled activation of host's innate and adaptive ($CD4^+$ T cell) immune responses (2, 15–21). Among interferons (IFNs), IFN-α/β and IFN-λ act as the first layer of anti-viral defense against corneal HSV-1 infection (1, 22–26). HSV-1 infected epithelial cells and infiltrated immune cells such as macrophages produce copious amounts of IFNs to induce robust anti-viral responses (2, 27). Macrophages control HSV-1 replication in the cornea through phagocytosis of infected epithelial cells and apoptotic neutrophils, followed by direct virucidal activities in the phagolysosomal compartment (19, 28). Moreover, macrophages, along with dendritic cells (DCs), also serve as Antigen-presenting cells (APCs) and prime naïve $CD4^+$ and $CD8^+$ T cells to initiate adaptive immune responses (29–31). Accordingly, our and others' past studies indicate that HSK lesions are mainly orchestrated by IFN-γ producing $CD4^+$ T cells (Th1) and to a lesser extent by interleukin IL-$17A^+CD4^+$ T cells (Th17) recognizing virus-derived peptides or unmasked self-antigens in the damaged cornea (15, 16, 21). Moreover, past studies have identified $Foxp3^+CD4^+$ regulatory T cells (Tregs)-mediated protection during HSK progression (17, 18). However, the contribution and molecular mechanisms of HSV-1 stimulated macrophages in Ag presentation to naïve $CD4^+$ T cells, and induction of effector Th1/Th17 versus regulatory T cell responses in HSK progression remains unknown.

In this study, we explored the role of IL-27, an immunoregulatory cytokine, after ocular HSV-1 infection and how it modulates macrophage-driven innate anti-viral and adaptive T cell responses. IL-27 plays both pro-viral and anti-viral roles through modulation of macrophages, DCs, $CD4^+$ and $CD8^+$ T cell effector functions during ongoing viral infection (32–40). Activated APCs such as DCs, macrophages, and inflammatory monocytes predominantly produce IL-27 (41–43). IL-27 binds to the heterodimeric IL-27 receptor that contains the IL-27Rα and gp130 subunits (42, 44–46). IL-27Rα is also called WSX-1 or TCCR (T cell cytokine receptor) and serves as the unique receptor for IL-27 (42, 44, 46). APCs not only synthesize IL-27 but also respond to IL-27 in an autocrine or paracrine manner (44, 47). In this study, we show that ocular HSV-1 infection induces IL-27 in the cornea, and macrophages could act as a source of IL-27 during the early phase of HSV-1 replication. Further, we demonstrated that IL-27 is critical for limiting HSV-1 shedding from the cornea, HSK progression, and corneal immunopathology. Accordingly, HSV-1 infection of IL-27Rα knock-out mice (IL-$27R\alpha^{-/-}$) showed significantly high HSV-1 titers in the tear film and were more susceptible to HSK progression. Further, our *in vitro* data indicate that IL-27 is critical for the macrophage-driven anti-viral effector responses, including type I IFNs production and ISGs expression. Moreover, our *in vitro* data suggest that IL-27 is critical for macrophage survival, efficient viral killing, and Ag uptake. Collectively, our data

indicate that IL-27 plays anti-viral and anti-inflammatory role after ocular HSV-1 infection through the regulation of macrophage-mediated innate and adaptive immune responses.

Materials and Methods

Mice.

IL-27Rα$^{-/-}$ mice (stock # 018078) were purchased from Jackson Laboratories (Bar Harbor, ME) and bred in-house (45). Control C57BL/6NJ (WT) mice (stock # 005304) were purchased from Jackson Laboratories (Bar Harbor, ME). All animal procedures were approved by the Institutional Animal Care and Use Committee (IACUC) of Auburn University. Male and female mice were bred and housed in Association for Assessment and Accreditation of Laboratory Animal Care (AAALAC) approved animal facilities. Mice were handled under a Biosafety Level-II cabinet. We used age and gender-matched, 6 to 8 weeks old mice for this study.

Viruses and cell lines.

HSV-1/RE and HSV-1/KOS strain expressing GFP under the gC promoter (HSV-1/GFP) were kindly provided by Dr. Paul R. Kinchington, Department of Ophthalmology, The University of Pittsburgh (48). Vero cells were used to culture and quantify HSV-1 by plaque assay. The viruses were aliquoted and stored at −80°C until further use. MK/T-1 (immortalized corneal fibroblast) cells were kindly provided by Dr. Noorjahan Panjwani, Department of Ophthalmology, Tufts University. Vero, MK/T-1 and L929 cells were maintained in DMEM media supplemented with 10% fetal bovine serum (FBS) at 37°C with 5% CO_2. HSV-1 virus infection *in vitro* was performed in serum-free DMEM for 2 hours, after which the cells were maintained in media with 2% FBS.

Antibodies and reagents.

The conjugated antibodies for flow cytometric analysis such as CD45-eFluor 450 (30-F11), Ly-6G-PE (1A8-Ly6g), Ly6C-Alexa fluor 488 (HK1.4), CD11c-APC (N418), F4/80-APC (BM8), CD11b-PerCP-Cyanine5.5 (M1/70), MHC-II-PerCP-eFlour710 (M5/114.15.2), CD4-APC (GK1.5), IFN-γ-FITC (XMG1.2), and unconjugated CD16/CD32 (93) were purchased from eBioscience™, Thermo Fisher Scientific. CD80-Brilliant violet 421™ (16–10A1), CD86-PE (PO3), CD40-FITC (3/23) and respective isotypes, CD8-Pacific blue (53–6.7), were purchased from Biolegend®. IL-27-p28-Alexa Fluor® 647 (Clone # 355025) was purchased from R&D systems. The LIVE/DEAD™ Fixable Yellow Dead Cell Stain Kit (Invitrogen, Catalog # L34968) was used to exclude dead cells in flow cytometry analyses.

Bone marrow-derived macrophage (BMDM) and dendritic cells (BMDC) culture.

Bone marrow (BM) cells were isolated from the femur and tibia of WT and IL-27Rα$^{-/-}$ mice. For obtaining a single cell suspension, BM cells were passed through a 23-gauge needle, two to three times. BM cells were then treated with ACK lysis buffer (Lonza) to lyse red blood cells, which were subsequently filtered through a 70 μm cell strainer. Further, the BM cells were cultured for 7 days in RPMI 1640 media supplemented with 20 % L929 conditioned media, and 10% FBS, as described previously (49). The culture medium was replenished every third day. The adherent cells were collected on day 7 and examined for

macrophage markers ($CD11b^+F4/80^+$) by flow cytometry. Similarly, for obtaining BMDC, BM cells from WT and IL-27R$\alpha^{-/-}$ mice were cultured in RPMI 1640 media supplemented with 10 ng/ml GM-CSF, 5 ng/ml IL-4 , and 10% FBS as described previously (50). The loosely adherent cells were collected on day 7 and examined for dendritic cell markers ($CD11c^+MHC\text{-}II^+$). The BMDM and BMDC were then stimulated with 2 multiplicity of infection (MOI) of HSV-1 for 24 hours, and were used for RNA and flow cytometry analysis.

Corneal HSV infection and Clinical scoring.

Corneal infection of WT and IL-27R$\alpha^{-/-}$ mice was conducted under deep anesthesia induced by intraperitoneal injection of ketamine (100 mg/kg) and xylazine (10 mg/kg). Further, the cornea was scarified using a 27-gauge needle, and 3 μl of phosphate buffered saline (PBS) containing 1×10^4 plaque-forming units (PFU) of HSV-1 was applied to the scarified eye. The eyes were examined on days 8, 11, and 14 post-infection (pi) using a slit lamp biomicroscope (Kowa Pharmaceuticals). HSK lesions were clinically scored with a scale of 0–5, in a blinded manner (22, 51). Briefly, the scoring system was as follows: lesion score of 0, normal cornea; +1, mild corneal haze; +2, moderate corneal scarring, iris visible; +3, severe haze, iris not visible; +4, severe haze and corneal ulcer; +5, corneal rupture and necrotizing keratitis. Further, the eye images were captured on day 14 pi using a stereomicroscope attached to a camera to visualize the severity of HSK.

Cell surface and intracellular cytokine staining.

HSV-1 infected corneas were collected from WT and IL-27R$\alpha^{-/-}$ mice at indicated days pi. Three to four corneas were pooled groupwise and treated with 5 mg/mL collagenase type IV (Gibco) and 0.1 mg/mL DNase (Worthington) for 30 minutes at 37 °C with 5% CO_2 for extracellular matrix digestion. After incubation, the corneas were crushed using a syringe plunger and passed through a 100 μm filter (Fisher Brand) for making a single cell suspension. For isolating the single cells from draining lymph nodes (DLN) and spleen, the tissue was crushed with a syringe plunger and passed through a 100 μm filter. Red blood cells were lysed in splenocytes using ACK lysis buffer (Lonza). The single-cell suspensions of the cornea, DLN, and spleen were resuspended in media and used for further staining. The LIVE/DEAD™ Fixable Yellow Dead Cell Stain Kit (Invitrogen, Catalog # L34968) was used per the manufacturer's instruction to determine the viability of cells. Further, the cells were blocked with unconjugated CD32/CD16 for 20 minutes in the staining buffer (PBS; 2 mM EDTA supplemented with 2% FBS). Antibody cocktail was added to the cells depending on each cell type and incubated for 30 minutes on ice. For $CD4^+$ T cell staining, CD4-APC (GK1.5) and CD45-eFluor 450 (30-F11) were used. For neutrophils ($CD45^+F4/80^-CD11b^+Ly6G^+$), CD45-eFluor 450 (30-F11), Ly-6G-PE (1A8-Ly6g), F4/80-APC (BM8), CD11b-PerCP-Cyanine5.5 (M1/70) were used. For inflammatory monocytes ($CD45^+CD11b^+Ly6C^+$), CD45-eFluor 450 (30-F11) and Ly6C-Alexa flour 488 (HK 1.4) were used. Intracellular cytokine staining (ICS) was used for staining IL-27 producing macrophages ($CD11b^+F4/80^+IL\text{-}27^+$), Th1 ($CD4^+IFN\text{-}\gamma^+$) and $CD8^+IFN\text{-}\gamma^+$ effector T cells. For IL-27 staining of corneal macrophages, cells were stimulated with UV-inactivated HSV-1 for 24 hours whereas for effector $CD4^+$ and $CD8^+$ T cells staining, cells were stimulated with cell stimulation cocktail containing PMA/

ionomycin with protein transport inhibitors (eBioscience™, Catalog # 00-4975-03) for 5 hours. The cells were fixed and permeabilized using Fixation permeabilization buffer set (eBioscience™, Catalog # 88-8824-00) according to the manufacturer's instructions and then stained with CD11b-PerCP-Cyanine5.5 (M1/70), F4/80-APC (BM8), and IL-27-p28 Alexa Fluor® 647 (Clone # 355025) for macrophages producing IL-27. Similarly for Th1 cells staining, CD4-APC (GK1.5) and IFN-γ-FITC (XMG1.2) was used and for $CD8^+$ effector T cells, CD8-Pacific blue (53–6.7) and IFN-γ-FITC (XMG1.2) was used. To quantify the Tregs ($CD4^+Foxp3^+$), cell surface staining with CD4-APC (GK1.5) was done, followed by intranuclear staining using the Foxp3/Transcription Factor Staining Buffer Set (eBioscience™, Catalog # 00-5523-00). The stained samples were acquired with BD™ LSR II flow cytometer and the data were analyzed using FlowJo software (Tree Star, Ashland, OR).

ELISA.

The cell supernatants were collected after centrifugation and used to measure the cytokine level by IL-27 sandwich ELISA (Invitrogen, Catalog # 88-7274-88) according to the manufacturer's protocol. The single-cell suspensions of DLN and spleen cells were collected from WT and IL-27Rα$^{-/-}$ mice infected with HSV-1 and re-stimulated with UV-inactivated HSV-1 for 24 hours. After centrifugation, the cell supernatant was subjected to cytokine analysis by IFN-γ sandwich ELISA (Invitrogen, Catalog # 88-7314-88) according to the manufacturer's protocol.

Viral titration.

HSV-1 levels in the tear film of infected mice on days 1, 3, and 5 pi were quantified using the eye-swab method (22). Briefly, the infected eyes were swabbed with sterile cotton tips soaked in serum-free sterile DMEM and stored at −80°C until further use. HSV-1 titers from WT and IL-27Rα$^{-/-}$ BMDM were determined by collecting the culture supernatants after 24 hours of infection. Further, required dilutions were made and quantified by plaque assay using Vero cells (52). Briefly, Vero cells were infected with diluted HSV-1 virus from the swabs or the BMDM cell culture supernatant and incubated at 37 °C with 5% CO_2 for 1–2 hours. After the incubation period, the virus-containing media was replaced with 1.5% carboxymethylcellulose (Thermo Scientific Chemicals) supplemented with 2% FBS. It was further incubated up to three days to allow plaque formation. Once plaques were observed under the microscope, the cells were fixed with 4% formaldehyde and stained with 0.01% crystal violet. Plaques were counted visually to determine HSV-1 titers.

Quantitative Real-Time PCR.

The corneas from uninfected or HSV-1 infected mice were homogenized at indicated time points, and total mRNA was extracted using TRIzol™ reagent (Invitrogen). BMDM or BMDC (5×10^5 cells per well) were stimulated with or without HSV-1 (2 MOI) for 24 hours. After incubation, the total mRNA was extracted using the PureLink RNA Mini kit (Invitrogen). RNA was reverse transcribed using a High-Capacity cDNA reverse transcription kit (Applied Biosystems), and the resulting cDNA was amplified by qPCRBIO SyGreen Blue mix Lo-ROX (Genesee Scientific). GAPDH was used for normalization, and relative gene expression was calculated using the

$2^{-\Delta\Delta Ct}$ method. The primers used for quantitative real-time PCR (qRT-PCR) were GAPDH-F5'-ATGTTCGTGATGGGTGTGAA-3', R5'-CTGTCTTCGTGTGTGGCTGT-3'; IL27p28- F5'-CTGAATCTCGATTGCCAGGAGTGA-3', R5'-AGCGAGGAAGCAGAGTCTCTCAGAG-3', IFN-β- F5'-CCTCAACCAGATCCAGCATT-3', R5'-GGATGAGGCTGTGAGAGGAG-3', ISG-15-F5'- GGTGTCCGTGACTAACTCCAT-3', R5'-TGGAAAGGGTAAGACCGTCCT-3', USP18- F5'- CAGACGTGTTGCCTTAACTCC-3', R5'-ACTCCGAGGCACTGTTATCC-3' HSV-1 gB-F5'-CGCATCAAGACCACCTCCTC-3', R5'- AGCTTGCGGGCCTCGTT.

Phagocytosis assay.

For measuring the phagocytic capacity of macrophages, MK/T-1 cells were infected with the 1 MOI of HSV-1/GFP virus for 24 hours. Infection of MK/T-1 cells by HSV-1/GFP was confirmed by observing green fluorescence under the fluorescent microscope. The infected MK/T-1 cells were centrifuged, washed with PBS, followed by co-culture with WT and IL-27Rα$^{-/-}$ BMDMs in a 1:2 ratio for 24 hours. Further, BMDM cells were stained with CD11b- PerCP-Cyanine5.5 (M1/70) and analyzed by flow cytometry. GFP^{+} signal in CD11b^{+} cells were considered as phagocytosis of infected MK/T-1 cells. Co-culture of BMDM with uninfected MK/T-1 cells and direct addition of HSV-1/GFP to BMDM cells were used as additional controls.

Apoptosis assay.

BMDMs from WT and IL-27Rα$^{-/-}$ mice were stimulated with HSV-1 for 24 hours and followed by annexin V/propidium iodide (PI) staining using kit (BD Biosciences, Catalog # 556547) according to the manufacturer's protocol. Annexin^{high}PI^{+} cells were considered as the late apoptotic or dead cells. The samples were kept on ice and acquired immediately using BD™ LSR II flow cytometer and the data were analyzed using FlowJo software (Tree Star, Ashland, OR).

Histopathology.

For Hematoxylin and Eosin (H&E) staining, the eyeballs from uninfected or HSV-1 infected WT and IL-27Rα$^{-/-}$ mice were collected at day 15 pi in Davidson's fixative solution. The eyeballs were embedded in paraffin blocks and the tissue sections were cut with a thickness of 6 μm and stained with H&E. The slides were viewed under a bright field microscope, and a board-certified pathologist performed histopathological analysis.

Statistics.

Statistical analysis of all *in vitro* and *in vivo* experiments was computed using GraphPad Prism 8 software (San Diego, CA). Statistical significance was computed by one-way ANOVA followed by Dunnett's multiple comparisons test to compare multiple groups. For comparing two groups, Student's t test (parametric) or Mann-Whitney U test (non-parametric) was used. Data are presented as means ± SEM. Each experiment was repeated a minimum of two to three times with significance reported at *$p \leq 0.05$, **$p \leq 0.01$, and ***$p \leq 0.001$.

Results

HSV-1 infection promotes IL-27 response in the cornea

IL-27 modulates innate and adaptive immune responses during viral and chronic inflammatory conditions (42, 53). Past studies have shown that IL-27 promotes viral clearance through modulation of macrophages, DCs, and $CD4^+$ and $CD8^+$ T cells-mediated effector responses during viral infections (32–39). However, the induction of IL-27, the molecular and cellular targets, and IL-27-mediated regulation of innate and adaptive immune responses after corneal HSV-1 infection is poorly defined. Thus, to investigate the role of IL-27 during ongoing corneal HSV-1 infection, we infected WT mice corneas with HSV-1 and isolated mRNA from infected corneas at indicated time points. As evident in Fig. 1A, IL-27 expression increased on days 1 and 2 pi with a decrease on day 3 pi. These data indicate that early HSV-1 replication, which peaks around day 2 pi after primary infection (19), promotes IL-27 response in the cornea. Since macrophages play a critical role in limiting HSV-1 replication in the cornea (27, 28) and could act as a source of IL-27 (43), we measured IL-27 production by infiltrated macrophages in the cornea and BMDM after HSV-1 infection. As shown in Fig 1B, macrophages infiltrated in the cornea showed IL-27 expression (Figure 1B). Similarly, *in vitro* infection of WT BMDM with HSV-1 resulted in significant induction of IL-27p28 mRNA and cytokine expression compared to uninfected BMDM (Fig. 1C, 1D). Further, HSV-1 stimulation of macrophages significantly induced IL-27Rα mRNA expression in macrophages (Fig. 1E). Collectively, our data indicate that HSV-1 infection promotes IL-27 response in the cornea, with macrophages acting as a possible source and target for IL-27 during HSV-1 replication phase.

IL-27 suppresses HSK progression

Past studies have shown that IL-27 plays either anti-viral or pro-viral role during various viral infections (35, 36, 53–55). However, the role of IL-27 during ocular HSV-1 infection is incompletely understood. Thus to further elucidate the role of IL-27 during HSK progression, we infected WT and IL-27Rα$^{-/-}$ corneas with HSV-1 and monitored the severity of HSK lesions over 15 days pi. As shown in Fig. 2A, the HSK lesion severity differed significantly on day 14 pi out of all tested time points (days 8, 11, and 14 pi). The absence of IL-27 receptor-mediated signaling in mice resulted in increased HSK lesion severity than in WT mice (Fig. 2A). The normal cornea is avascular (Fig.2B, left panel) and employs numerous immune suppressive mechanisms to achieve corneal transparency (2, 56, 57). However, HSV-1 infection promotes infiltration of immune cells that cause opacity in the cornea, with peak severity reaching around day 15 pi in the primary ocular HSV-1 infection model (Fig. 2B, middle panel). We noted increased gross HSK lesion severity in IL-27Rα$^{-/-}$ mice (Fig. 2B, right panel) compared to WT mice (Fig. 2B, middle panel). Next, we euthanized mice on day 15 pi from WT and IL-27Rα$^{-/-}$ groups to evaluate the histopathological changes and immune cell infiltration in the cornea by performing H&E staining. Consistent with the gross HSK lesion severity score, WT corneas showed significant infiltration of leukocytes in the stromal layers with resultant thickening of corneal stroma on day 15 pi (Fig. 2B, bottom middle panel) compared to uninfected mice (Fig. 2B, bottom left panel). In contrast to WT corneas, IL-27Rα$^{-/-}$ mice corneas showed a complete erosion of corneal epithelial layers, hyperkeratosis (epidermization), and extensive stromal

fibrosis after HSV-1 infection (Fig. 2B, bottom right panel). Collectively, these data indicate that the optimum induction of IL-27-mediated responses after HSV-1 infection are critical for limiting HSK lesion progression.

IL-27 modulates inflammatory immune responses in the cornea after HSV-1 infection

The inflammatory immune cells such as neutrophils and $CD4^+$ effector T cells are absent in the corneal stroma of naïve uninfected mice. However, neutrophils infiltrate the cornea during early and later stages of HSK and secrete inflammatory cytokines, MMPs, and VEGF-A that cause damage to the corneal tissue architecture and promote angiogenesis during HSK progression (15, 16, 58, 59). Since the absence of IL-27-mediated signaling in mice enhanced HSK lesion severity, we investigated whether IL-27 modulates neutrophil responses in the cornea at day 15 pi. As shown in Fig. 3, we noted an increased infiltration of total leukocytes (Fig. 3A, 3C) and neutrophils (Fig 3B, 3C, Supplemental Fig.1 for gating strategy) in the corneas of IL-27R$\alpha^{-/-}$ mice compared to WT mice. Our prior studies have shown that $CD4^+$ effector T cells (Th1 and Th17) play a central role in orchestrating HSK pathology in the cornea (15, 18). Among effector $CD4^+$ T cells, Th1 cells play a dominant role in mediating HSK pathology (15, 21). Thus, we investigated whether increased HSK pathology in IL-27R$\alpha^{-/-}$ mice is due to changes in $CD4^+$ and Th1 effector T cell responses in the cornea. The frequencies and total numbers of $CD4^+$ (Fig. 3D, 3F) and IFN-γ^+ producing $CD4^+$ T cells (Fig. 3E, 3F) were higher in IL-27R$\alpha^{-/-}$ mice corneas compared to WT mice. These data suggest that IL-27 plays a critical regulatory role in suppressing HSK pathology through modulation of Th1 and neutrophils-mediated inflammatory responses in the cornea.

IL-27 is required for optimum Th1 responses in the secondary lymphoid organs after corneal HSV-1 infection

Past studies in a murine model of primary corneal HSV-1 infection indicate that HSK lesions are primarily orchestrated by Th1 cells that recognize viral peptides or unmasked self-antigens in the damaged cornea (1, 21). Furthermore, our previous studies have shown that corneal HSV-1 infection elicits not only Th1 but also Th17 and regulatory T cell responses in the DLN and spleen (15, 17). Since we noted significantly increased infiltration of Th1 cells in the corneas of IL-27R$\alpha^{-/-}$ mice, we elucidated whether IL-27 regulates Th1 responses in the DLN and spleen after corneal HSV-1 infection. In contrast to the cornea, we noted a significant reduction in the percentage of Th1 cells in the DLN and spleen (Fig. 4A, 4B) of IL-27R$\alpha^{-/-}$ mice compared to control animals on day 15 pi. Similarly, there was a significant reduction in the total numbers of Th1 cells in the DLN and spleen (Fig. 4C) of IL-27R$\alpha^{-/-}$ mice compared to WT mice. We also noted a significant reduction in IFN-γ production by *ex vivo* stimulated DLN and spleen cells (Fig. 4D). However, Treg percentages and total numbers were unchanged between IL-27R$\alpha^{-/-}$ and WT mice (Fig. 4E–G). These data indicate that IL-27 is critical for differentiation of naïve $CD4^+$ T cells to effector Th1 cells after corneal HSV-1 infection.

IL-27 modulates Ag uptake and maturation of APCs after HSV-1 infection

The diminished Th1 responses in secondary lymphoid organs of IL-27R$\alpha^{-/-}$ mice after HSV-1 indicate a possible T-cell intrinsic or APCs (DCs and macrophage)-mediated defects

in the differentiation of naïve $CD4^+$ T cells to Th1 cells. Past studies have shown that IL-27 and IL-12 synergistically promote Th1 differentiation and IFN-γ production by Th1 cells (42, 44, 60). Since $CD4^+$ T cells intrinsic role of IL-27 in Th1 differentiation is well established, we investigated whether IL-27 modulates APCs to regulate Th1 cell responses after HSV-1 infection. APCs control the fate of naïve T cell differentiation by regulating Ag-uptake, Ag-processing, Ag-presentation, the activation of pathogen-specific Toll-like receptors (TLRs), and differential secretion of T cell subset polarizing cytokines (61, 62). Furthermore, the expression of activation markers such as CD80 and CD86 on APCs is critical for CD28-mediated co-stimulation of naïve T cells that drives increased survival, metabolism, and differentiation of activated T cells (63). Additionally, accessory T cell activation signals include the expression of CD40 on APCs, which engages with the CD40L expressed on the T cells (64, 65). CD40/CD40L interaction further activates the APCs to produce IL-12 which skews the differentiation of naïve T cells into Th1 (64, 65). To investigate the role of IL-27 in APCs-mediated regulation of T cell responses, we differentiated BM cells from naïve WT and IL-27Rα$^{-/-}$ mice to BMDCs using GMCSF and IL-4, followed by stimulation with HSV-1. As shown in Fig. 5A, and 5B, we noted a significantly reduced expression of CD80, CD86, CD40 and MHC-II on BMDCs from IL-27Rα$^{-/-}$ mice compared to WT BMDCs. In addition to phagocytosis and killing of ingested pathogens, macrophages can also serve as APCs (66). Since macrophages play a central role in HSV-1 killing and control of virus replication in the cornea (28), we investigated whether IL-27 regulates the activation of macrophages after HSV-1 infection. Similar to BMDCs, the HSV-1 stimulation from IL-27Rα$^{-/-}$ BMDMs showed a significant reduction in CD80, CD86, and CD40 expression compared to WT BMDMs (Fig. 5C, 5D). Next, we investigated whether the reduced expression of activation markers was due to a defect in Ag uptake by macrophages in the absence of IL-27 signaling. As shown in Fig. 5E, and 5F, IL-27Rα$^{-/-}$ BMDMs showed a significantly reduced uptake of HSV-1 infected corneal stromal fibroblasts compared to WT BMDMs, indicating that IL-27 is crucial for APCs-mediated HSV-1 uptake, Ag processing and presentation to naïve $CD4^+$ T cells. Our results are consistent with an earlier study where the authors showed that IL-27 is required for effective Ag processing and presentation to T cells by monocyte-derived DCs (67). These data suggest that the IL-27-mediated responses in APCs are critical for efficient HSV-1 phagocytosis, Ag processing and presentation, maturation and differentiation of naïve $CD4^+$ T cells.

IL-27 is required for maturation of APCs and induction of optimum Th1 responses in the secondary lymphoid organs after corneal HSV-1 infection

Immature DCs acquire antigen from cornea and then migrate to secondary lymphoid organs, undergo maturation and effectively present processed peptides to Ag-specific T cells in the secondary lymphoid organs (68, 69). During maturation, DCs upregulate variety of receptors, particularly expression of Ag-bearing MHC-II molecules on cell surface (70). Since we observed reduced expression of co-stimulatory ligands and MHC-II expression in IL-27Rα$^{-/-}$ BMDC, we examined the expression of MHC-II by DCs in the DLNs on day 2 pi after corneal HSV-1 infection. Similar to BMDCs, the expression of MHC-II on $CD11c^+$ cells of DLNs were significantly reduced in IL-27Rα$^{-/-}$ mice compared to the control HSV-1 infected mice (Fig. 6A, 6B). $CD4^+$ effector T cells are fully apparent in the

DLNs by day 6–8 pi with continued infiltration to cornea as HSK progresses (15). Further to confirm whether reduced MHC-II expression in the absence of IL-27 signaling regulates the induction of T cell responses, we examined the Th1 responses in the DLN and spleen on day 8 pi. Similar to the data presented in Figure 4, we noted a marked decrease in percentage of Th1 cells in IL-27Rα$^{-/-}$ mice compared to the WT mice after HSV-1 infection (Fig. 6C, 6D). In contrast, we did not observe a significant change in the IFN-γ producing CD8^{+} T cells in the DLN and spleen of WT and IL-27Rα$^{-/-}$ mice (Fig. 6E, 6F). Collectively, our data indicate that IL-27 is critical for the maturation of APCs and induction of optimum Th1 responses in DLNs during early phase of corneal HSV-1 infection.

IL-27 regulates HSV-1 replication and early innate immune responses in the cornea

The initial virus replication in the corneal epithelium and resultant uncontrolled activation of innate and adaptive immune responses play a central role in HSK immunopathology (2, 19). Since the absence of IL-27-mediated signaling in mice exacerbated HSK lesion severity (Fig. 2A), we next investigated whether increased HSK pathology in IL-27Rα$^{-/-}$ mice is due to increased HSV-1 replication and defects in innate anti-viral responses during the early stages of HSV-1 infection. First, we measured viral titers in the tear film collected from HSV-1 infected WT and IL-27Rα$^{-/-}$ corneas on various days pi. As shown in Fig. 7A, the absence of IL-27-mediated responses after corneal HSV-1 infection resulted in increased HSV-1 replication and significantly increased viral titers in the tear film on day 5 pi compared to WT mice. We did not observe any lag in HSV-1 shedding in both WT and IL-27Rα$^{-/-}$ corneas as there was no detectable virus by day 8 pi (Fig. 7A). The innate immune cells, including neutrophils and macrophages, play a critical role in the initial clearance of HSV-1 from the cornea (22, 28). However, the excessive infiltration of these cells, followed by increased secretion of effector anti-viral and inflammatory cytokines, causes irreversible corneal tissue damage and opacity (1, 6, 71). Accordingly, we noted significantly increased infiltration of total leukocytes (Fig. 7B, 7D), neutrophils, and macrophages (Fig. 7C, 7D) in the corneas of IL-27Rα$^{-/-}$ mice compared to WT mice on day 2 pi. Despite increased infiltration of neutrophils and macrophages in HSV-1 infected IL-27Rα$^{-/-}$ cornea (Fig. 7B–D), we noted significantly higher viral titers compared to control mice (Fig. 7A). These data suggest that infiltrated macrophages are inefficient in HSV-1 killing in the absence of IL-27-mediated innate immune responses.

IL-27 is indispensable for the efficient induction of macrophage-intrinsic anti-viral responses after HSV-1 infection

Macrophages play a critical role in the initial clearance of HSV-1 (2, 19). Specifically, macrophages control HSV-1 replication in the cornea through phagocytosis of infected epithelial cells and apoptotic neutrophils, followed by direct virucidal activities in the phagolysosomal compartment (2, 19, 28). The increased susceptibility to HSK and elevated viral titers in the tear film of IL-27Rα$^{-/-}$ mice indicates a possible protective role of IL-27 through modulation of macrophage-intrinsic virucidal and anti-viral immune responses after HSV-1 infection. To delineate macrophage-intrinsic IL-27-mediated anti-HSV-1 responses, we stimulated BMDMs with HSV-1 and quantified viral titers in cell supernatants using plaque assay and measured HSV-1 gB in cells using mRNA quantification. As shown in Fig. 8A, we noted an increased viral titer in IL-27Rα$^{-/-}$ BMDMs cell supernatant compared

to WT BMDMs cell supernatant. Similarly, there was a significant increase in HSV-1 gB mRNA expression in IL-27Rα$^{-/-}$ BMDMs compared to the WT BMDMs (Fig. 8B). The increase in viral titers observed in IL-27Rα$^{-/-}$ BMDM could be explained by impaired phagocytosis, decrease in macrophage survival and reduced IFN responses after HSV-1 infection. As shown earlier in Fig. 5E, we observed decrease in phagocytosis of infected corneal fibroblast cells by IL-27Rα$^{-/-}$ macrophages. Next, we tested whether absence of IL-27 signaling regulates the macrophage survival after HSV-1 infection. We infected WT and IL-27Rα$^{-/-}$ BMDMs with HSV-1 and analyzed cell death using flow cytometry. Our data show a significant increase in late apoptosis (Annexin-V^{+}PI^{+} cells) of BMDMs without IL-27 signaling (Fig. 8C, 8D). Type I IFNs induce a robust anti-viral state and protect infected and nearby uninfected cells from viral infection, cytopathic effects, and cell killing (24). Past studies have shown that IL-27 regulates type-I IFN responses and acts synergistically to control viruses' spread (53, 72–74). Therefore, we investigated whether increased HSV-1 titers in the tear film and BMDMs from IL-27Rα$^{-/-}$ mice are due to defects in type I IFN production and downstream ISG expression. We noted a significant decrease in mRNA expression and IFN-β production from IL-27Rα$^{-/-}$ BMDMs than in WT BMDMs (Fig. 8E, 8F). Type I IFNs induce many ISGs to promote an antiviral state after HSV-1 infection (1). Among the various ISGs, ISG-15 promotes ISGylation of IRF3 and USP-18 stabilizes STING which are critical for further promoting type-I IFNs and inhibiting HSV-1 replication (75, 76). We observed a significant reduction in the expression of ISG-15 and USP-18 by BMDMs in the absence of IL-27 receptor-mediated signaling (Fig. 8G). Similarly, we observed significant reduction in ISG-15 and USP-18 expression in IL-27Rα$^{-/-}$ cornea on day 2 pi when compared to WT cornea (Figure 8H). Collectively, these data suggest that IL-27 regulates HSV-1 replication and killing through macrophage survival, production of type I IFNs and ISGs after HSV-1 infection.

Discussion

Absolute corneal transparency is requisite for normal vision. However, the recurrent episodes of HSV-1 infection in the cornea cause a very painful and vision-impairing immunopathology (77). The HSK progression is primarily driven by lytic HSV-1 replication in the corneal epithelium, followed by uncontrolled activation of innate and adaptive immune responses (77). There is an urgent need for immunotherapy-based approaches as current anti-viral and corticosteroid-based remedies, are partially effective, and have many side effects (11, 13). Thus, understanding the host's innate defense mechanisms that mount strong anti-viral responses without causing overt activation of the immune system holds the key to developing novel immunotherapies to treat HSK. In this study, we investigated whether HSV-1 regulates IL-27 responses in the cornea and IL-27-mediated regulation of innate and adaptive immune responses during HSK progression. Our results show that corneal HSV-1 infection promotes macrophage-mediated IL-27 expression. The *in vitro* infection of BMDMs showed a marked increased production of IL-27, indicating that resident and infiltrating monocytes or macrophages in the cornea act as a source of IL-27 after HSV-1 infection. Using a murine model of primary corneal HSV-1 infection and IL-27Rα$^{-/-}$ mice, we demonstrate that IL-27 is critical for suppressing HSK progression and inflammatory responses in the cornea. The mice lacking IL-27 receptor-mediated signaling

showed marked infiltration of Th1 cells and neutrophils which cause damage to the cornea and promote HSK lesions. Further, *in vitro* mechanistic investigations revealed that IL-27 is essential for macrophage-mediated HSV-1 phagocytosis, IFN-β production, optimum anti-HSV-1 ISGs expression, and HSV-1 killing. Additionally, we noted a significant increase in the apoptosis of HSV-1 infected IL-27Rα$^{-/-}$ macrophages compared to control macrophages suggesting the critical role of IL-27 in promoting macrophage-mediated anti-HSV-1 responses. Moreover, IL-27Rα$^{-/-}$ macrophages and DCs showed reduced expression of co-stimulatory markers, a likely downstream effect of reduced phagocytosis (Ag uptake). Collectively, this resulted in significantly increased shedding of HSV-1 from cornea of IL-27Rα$^{-/-}$ mice leading to increased HSK. Our results indicate that IL-27 induces a strong endogenous anti-viral state and suppresses inflammatory responses. Thus, promoting IL-27-mediated responses could be a promising therapeutic approach to prevent recurrent corneal HSV-1 infection and associated HSK pathology.

IL-27 is a pleiotropic immunoregulatory cytokine belonging to the IL-12 family of cytokines (78). Pathogen-activated DCs, macrophages, and inflammatory monocytes predominantly produce IL-27 (43, 44, 79). IL-27 plays both pro- and anti-viral roles by regulating innate and adaptive immune responses (35, 36, 53–55). Past studies have shown that IL-27 is expressed by virus stimulated-PBMCs and monocyte-derived macrophages, and IL-27 treatment inhibited HIV-1 replication in CD4^{+} T cells and myeloid cells (74, 80). Similarly, our data indicate that HSV-1 significantly induces IL-27 production in macrophages (Fig. 1). The *in vivo* protective anti-HSV-1 role of IL-27 was further confirmed by increased shedding of virus from the cornea of HSV-1 infected mice lacking IL-27 receptor-mediated signaling (Fig. 7). IL-27 activates Janus activated kinase (JAK) 1 or 2, followed by downstream phosphorylation, activation, and translocation of signal transducer and activator of transcription STAT1 and STAT3 dimer in the nucleus (42, 44). Likewise, type I IFNs activate JAK1, followed by phosphorylation of STAT1 (81, 82). Interestingly, IL-27 and type I IFNs can cross-regulate the activation of downstream signaling events during viral infections (74, 83). Accordingly, our data show that IL-27 is critical for optimum induction of type I IFNs and ISGs by macrophages after HSV-1 infection (Fig. 8) and suggest that IL-27 positively regulates type I IFN-mediated anti-HSV-1 responses. Similarly, a recent study showed that IL-27 activates anti-viral protein response in the human epidermal keratinocytes after Zika virus infection by inducing JAK-STAT-1 and IRF3 signaling (53). This study demonstrated that IL-27 inhibits Zika virus replication, morbidity, and mortality after the cutaneous route of infection through increased expression of ISGs (53). HSV-1 has evolved numerous immune evasion strategies targeting type I IFNs (1). For example, HSV-1 viral proteins ICP27 and VP16 inhibit STAT1 phosphorylation and block IRF3 and IRF7 activation (84–86). These immune evasion mechanisms could promote efficient HSV-1 replication in the epithelial cells. However, HSV-1-infected macrophages could overcome these inhibitory mechanisms through increased IL-27 production and autocrine IL-27-mediated activation of STAT1 and IRFs to promote ISGs-mediated anti-viral responses. Our data indicate that IL-27 plays a critical role in macrophage survival after HSV-1 infection as the absence of IL-27-mediated responses significantly elevated apoptosis of HSV-1 infected macrophages.

Our prior studies have established the critical role of effector (Th1 and Th17) and Treg cells in HSK progression (15, 17, 18). IL-27 signaling is crucial for the differentiation and effector functions of both $CD4^+$ and $CD8^+$ T cells through the regulation of Tbet expression and IFN-γ production (87–89). Accordingly, our data suggest that IL-27 is critical for Th1 induction and IFN-γ production by T cells after corneal HSV-1 infection (Fig. 4 and 6). Further, we did not see a significant change in Treg percentages or total numbers in DLN and spleen after HSV-1 infection. Our data indicate that the reduced Th1 induction in the absence of IL-27Rα-mediated signaling could result from extrinsic defects in APCs or intrinsic IL-27-mediated defects in T cell differentiation (34, 44, 47). Also, type I IFNs regulate adaptive immunity through modulation of APCs (Ag uptake, maturation, and presentation) and T cell-mediated responses (90, 91). In addition to DCs, macrophages also serve as APCs and prime naïve $CD4^+$ T cells to induce effector T cell responses (29–31). Thus, the reduced Th1 responses in HSV-1 infected IL-27R$\alpha^{-/-}$ mice could result from reduced type I IFN production by macrophages and subsequent diminished Ag uptake and maturation. Indeed, we noted a significantly reduced production of type I IFNs by HSV-1 infected IL-27R$\alpha^{-/-}$ macrophages (Figure 8). Further, we observed a markedly diminished expression of co-stimulatory markers such as CD40, CD80, and CD86 in addition to decreased MHC-II cell surface expression by HSV-1 stimulated IL-27R$\alpha^{-/-}$ BMDCs (Fig. 5). An earlier report showed that IL-27 suppresses the Ag-presentation function of splenic DCs by reducing the expression of co-stimulatory markers after LPS stimulation (47). In contrast, Jung et al. showed that phagocytic capacity and Ag presentation by monocyte-derived human DCs are enhanced by IL-27 (67). In addition to BMDCs, we observed reduced co-stimulatory marker expression in IL-27R$\alpha^{-/-}$ BMDMs. Our *in vitro* co-culture experiments using WT and IL-27R$\alpha^{-/-}$ BMDMs with HSV-1- infected corneal stromal fibroblasts (MK/T-1) indicate that IL-27 is critical for efficient phagocytosis of infected cells (Ag uptake) and subsequent maturation of APCs (Fig. 5). DCs serve as professional APCs and regulate the Th1 responses during HSK progression (30, 62). Furthermore, IL-27 is known to modulate DCs maturation and induce immunosuppression through DCs- mediated differential induction of effector and regulatory T cell responses (47, 92). Accordingly, we observed decreased MHC-II expression on $CD11c^+$ cells in IL-27R$\alpha^{-/-}$ DLNs after day 2 pi (Fig 6). Collectively, our findings demonstrate that IL-27 could regulate Th1 responses directly through T-cell intrinsic mechanisms and indirectly through the regulation of type I IFNs, Ag uptake, and maturation of macrophages and DCs.

Apart from anti-viral functions, IL-27 also regulates the inflammatory responses through differential induction of Th1, Th2, Th17, Treg, and Tr1 cells (87, 93, 94). Furthermore, IL-27 regulates the induction of $CD4^+$ and $CD8^+$ T cell responses during viral infection, thereby modulating the severity of viral infections and associated pathologies (32, 34, 37). Past study showed that IL-27 inhibits lung immunopathology after influenza infection by regulating Th1, Th17, IL-10, and neutrophil responses (36). This study demonstrated that mice lacking IL-27Rα promoted IFN-γ and IL-17 production by T cells with subsequently increased infiltration of neutrophils in the lung after influenza virus infection (36). Similarly, we noted a significantly increased neutrophil infiltration in the cornea during early viral replication (day 2) and late stages of HSK (day 15) in HSV-1 infected IL-27R$\alpha^{-/-}$ mice. However, we noted a marked reduction of Th1 responses in the DLN with higher infiltration

of Th1 cells in the cornea of HSV-1 infected IL-27Rα$^{-/-}$ mice. This discrepancy is partially explained by increased HSV-1 titers in IL-27Rα$^{-/-}$ mice, diminished Th1 responses and IFN-γ production by Th1 cells without IL-27 signaling. The increased viral titers could drive increased migration of Th1 cells to the cornea from DLNs during early HSV-1 replication phase. Similarly, several other viral infection studies have reported the critical role of IL-27 in modulating immunopathology through differential regulation of effector CD4$^+$ and CD8$^+$ T cell responses (32, 33, 44, 54, 74). However, we did not observe any significant changes in the CD8$^+$ effector T cell response in the DLNs (day 8) after HSV-1 infection. Further studies are required to understand how IL-27 modulates specific effector T cells to promote antiviral and inflammatory responses during HSK progression.

Our findings collectively demonstrate that corneal HSV-1 infection induces IL-27 production by macrophages and IL-27 plays anti-viral and anti-inflammatory roles during the HSK progression. These data indicate the critical role of IL-27 in modulating macrophage-mediated HSV-1 killing, type I IFN induction, Ag uptake and presentation, and induction of Th1 responses after corneal HSV-1 infection. Further research is needed to delineate the role of IL-27-mediated signaling in APCs and T cells that regulate effector CD4$^+$ and CD8$^+$ T cell responses during ongoing HSV-1 infection. Also, it will be interesting to delineate the IL-27-mediated molecular mechanisms for differential Th1 responses in the DLN and cornea (site of inflammation) and whether IL-27 regulates the inflammation during later stages of HSK (when replicating virus is absent in the cornea) through regulation of Th1 cell migration and their cytokine production. Further, *in vivo* mechanistic studies using macrophages, CD4$^+$ T cells, and DCs-specific conditional deletion of IL-27Rα are needed to conclusively define the anti-viral and anti-inflammatory role of IL-27 during corneal HSV-1 infection and HSK progression. In conclusion, the anti-viral role of IL-27 during corneal HSV-1 infection and HSK progression could have broad therapeutic implications for patients suffering from recurrent HSK, the leading cause of infectious blindness in the US.

Supplementary Material

Refer to Web version on PubMed Central for supplementary material.

Acknowledgments

We thank Dr. Paul R. Kinchington, Department of Ophthalmology, The University of Pittsburgh for providing the HSV-1/GFP virus. We thank Dr. Noorjahan Panjwani, Department of Ophthalmology, Tufts University, for providing MK/T-1 cells for the phagocytosis assay. We thank Auburn University Histopathology and Flow Cytometry Core Facilities for support.

This work was supported by National Eye Institute Grant EY035057, National Institute of Allergy and Infectious Diseases Grant AI153794 to A.S. and Auburn University Presidential Graduate Research Fellowship to F.A.

References

1. Ren J, Antony F, Rouse BT, and Suryawanshi A. 2023. Role of Innate Interferon Responses at the Ocular Surface in Herpes Simplex Virus-1-Induced Herpetic Stromal Keratitis. Pathogens 12.
2. Gimenez F, Suryawanshi A, and Rouse BT. 2013. Pathogenesis of herpes stromal keratitis--a focus on corneal neovascularization. Prog Retin Eye Res 33: 1–9. [PubMed: 22892644]

3. Farooq AV, and Shukla D. 2012. Herpes simplex epithelial and stromal keratitis: an epidemiologic update. Surv Ophthalmol 57: 448–462. [PubMed: 22542912]
4. Koganti R, Yadavalli T, Naqvi RA, Shukla D, and Naqvi AR. 2021. Pathobiology and treatment of viral keratitis. Exp Eye Res 205.
5. Rowe AM, St Leger AJ, Jeon S, Dhaliwal DK, Knickelbein JE, and Hendricks RL. 2013. Herpes keratitis. Prog Retin Eye Res 32: 88–101. [PubMed: 22944008]
6. Wang L, Wang R, Xu C, and Zhou H. 2020. Pathogenesis of Herpes Stromal Keratitis: Immune Inflammatory Response Mediated by Inflammatory Regulators. Front Immunol 11: 766. [PubMed: 32477330]
7. James C, Harfouche M, Welton NJ, Turner KME, Abu-Raddad LJ, Gottlieb SL, and Looker KJ. 2020. Herpes simplex virus: global infection prevalence and incidence estimates, 2016. B World Health Organ 98: 315–329.
8. Liesegang TJ, Melton LJ, Daly PJ, and Ilstrup DM. 1989. Epidemiology of Ocular Herpes-Simplex - Incidence in Rochester, Minn, 1950 through 1982. Arch Ophthalmol-Chic 107: 1155–1159.
9. Holland EJ, and Schwartz GS. 1999. Classification of herpes simplex virus keratitis. Cornea 18: 144–154. [PubMed: 10090359]
10. Knickelbein JE, Hendricks RL, and Charukanmoetkanok P. 2009. Management of Herpes Simplex Virus Stromal Keratitis: An Evidence-based Review. Survey of Ophthalmology 54: 226–234. [PubMed: 19298901]
11. Azher TN, Yin XT, Tajfirouz D, Huang AJ, and Stuart PM. 2017. Herpes simplex keratitis: challenges in diagnosis and clinical management. Clin Ophthalmol 11: 185–191. [PubMed: 28176902]
12. Koganti R, Yadavalli T, and Shukla D. 2019. Current and Emerging Therapies for Ocular Herpes Simplex Virus Type-1 Infections. Microorganisms 7.
13. Tsatsos M, MacGregor C, Athanasiadis I, Moschos MM, Hossain P, and Anderson D. 2016. Herpes simplex virus keratitis: an update of the pathogenesis and current treatment with oral and topical antiviral agents. Clin Exp Ophthalmol 44: 824–837. [PubMed: 27273328]
14. Wilhelmus KR, Gee L, Hauck WW, Kurinij N, Dawson CR, Jones DB, Barron BA, Kaufman HE, Sugar J, Hyndiuk RA, Laibson PR, Stulting RD, and Asbell PA. 1994. Herpetic Eye Disease Study - a Controlled Trial of Topical Corticosteroids for Herpes-Simplex Stromal Keratitis. Ophthalmology 101: 1883–1895. [PubMed: 7997324]
15. Suryawanshi A, Veiga-Parga T, Rajasagi NK, Reddy PB, Sehrawat S, Sharma S, and Rouse BT. 2011. Role of IL-17 and Th17 cells in herpes simplex virus-induced corneal immunopathology. J Immunol 187: 1919–1930. [PubMed: 21765013]
16. Suryawanshi A, Veiga-Parga T, Reddy PB, Rajasagi NK, and Rouse BT. 2012. IL-17A differentially regulates corneal vascular endothelial growth factor (VEGF)-A and soluble VEGF receptor 1 expression and promotes corneal angiogenesis after herpes simplex virus infection. J Immunol 188: 3434–3446. [PubMed: 22379030]
17. Veiga-Parga T, Suryawanshi A, Mulik S, Gimenez F, Sharma S, Sparwasser T, and Rouse BT. 2012. On the role of regulatory T cells during viral-induced inflammatory lesions. J Immunol 189: 5924–5933. [PubMed: 23129753]
18. Veiga-Parga T, Suryawanshi A, and Rouse BT. 2011. Controlling viral immuno-inflammatory lesions by modulating aryl hydrocarbon receptor signaling. PLoS Pathog 7: e1002427. [PubMed: 22174686]
19. Biswas PS, and Rouse BT. 2005. Early events in HSV keratitis--setting the stage for a blinding disease. Microbes Infect 7: 799–810. [PubMed: 15857807]
20. Stuart PM, and Keadle TL. 2012. Recurrent herpetic stromal keratitis in mice: a model for studying human HSK. Clin Dev Immunol 2012: 728480. [PubMed: 22593769]
21. Niemialtowski MG, and Rouse BT. 1992. Predominance of Th1 cells in ocular tissues during herpetic stromal keratitis. J Immunol 149: 3035–3039. [PubMed: 1357034]
22. Antony F, Pundkar C, Sandey M, Jaiswal AK, Mishra A, Kumar A, Channappanavar R, and Suryawanshi A. 2021. IFN-lambda Regulates Neutrophil Biology to Suppress Inflammation in Herpes Simplex Virus-1-Induced Corneal Immunopathology. J Immunol 206: 1866–1877. [PubMed: 33811102]

23. Rasmussen SB, Sorensen LN, Malmgaard L, Ank N, Baines JD, Chen ZJ, and Paludan SR. 2007. Type I interferon production during herpes simplex virus infection is controlled by cell-type-specific viral recognition through Toll-like receptor 9, the mitochondrial antiviral signaling protein pathway, and novel recognition systems. J Virol 81: 13315–13324. [PubMed: 17913820]
24. Conrady CD, Jones H, Zheng M, and Carr DJ. 2011. A Functional Type I Interferon Pathway Drives Resistance to Cornea Herpes Simplex Virus Type 1 Infection by Recruitment of Leukocytes. J Biomed Res 25: 111–119. [PubMed: 21709805]
25. Conrady CD, Zheng M, Fitzgerald KA, Liu C, and Carr DJ. 2012. Resistance to HSV-1 infection in the epithelium resides with the novel innate sensor, IFI-16. Mucosal Immunol 5: 173–183. [PubMed: 22236996]
26. Zanoni I, Granucci F, and Broggi A. 2017. Interferon (IFN)-lambda Takes the Helm: Immunomodulatory Roles of Type III IFNs. Front Immunol 8: 1661. [PubMed: 29234323]
27. Conrady CD, Zheng M, Mandal NA, van Rooijen N, and Carr DJ. 2013. IFN-alpha-driven CCL2 production recruits inflammatory monocytes to infection site in mice. Mucosal Immunol 6: 45–55. [PubMed: 22692455]
28. Jeon S, Rowe AM, Carroll KL, Harvey SAK, and Hendricks RL. 2018. PD-L1/B7-H1 Inhibits Viral Clearance by Macrophages in HSV-1-Infected Corneas. J Immunol 200: 3711–3719. [PubMed: 29669784]
29. Muntjewerff EM, Meesters LD, and van den Bogaart G. 2020. Antigen Cross-Presentation by Macrophages. Frontiers in Immunology 11.
30. Hamrah P, Pavan-Langston D, and Dana R. 2009. Herpes simplex keratitis and dendritic cells at the crossroads: lessons from the past and a view into the future. Int Ophthalmol Clin 49: 53–62.
31. Lee DH, Jaggi U, and Ghiasi H. 2019. CCR2+ migratory macrophages with M1 status are the early-responders in the cornea of HSV-1 infected mice. PLoS One 14: e0215727. [PubMed: 30998796]
32. Huang Z, Zak J, Pratumchai I, Shaabani N, Vartabedian VF, Nguyen N, Wu T, Xiao C, and Teijaro JR. 2019. IL-27 promotes the expansion of self-renewing CD8(+) T cells in persistent viral infection. J Exp Med 216: 1791–1808. [PubMed: 31164392]
33. Harker JA, Wong KA, Dallari S, Bao P, Dolgoter A, Jo Y, Wehrens EJ, Macal M, and Zuniga EI. 2018. Interleukin-27R Signaling Mediates Early Viral Containment and Impacts Innate and Adaptive Immunity after Chronic Lymphocytic Choriomeningitis Virus Infection. J Virol 92.
34. Wehrens EJ, Wong KA, Gupta A, Khan A, Benedict CA, and Zuniga EI. 2018. IL-27 regulates the number, function and cytotoxic program of antiviral CD4 T cells and promotes cytomegalovirus persistence. PLoS One 13: e0201249. [PubMed: 30044874]
35. Muallem G, Wagage S, Sun Y, DeLong JH, Valenzuela A, Christian DA, Harms Pritchard G, Fang Q, Buza EL, Jain D, Elloso MM, Lopez CB, and Hunter CA. 2017. IL-27 Limits Type 2 Immunopathology Following Parainfluenza Virus Infection. PLoS Pathog 13: e1006173. [PubMed: 28129374]
36. Liu FD, Kenngott EE, Schroter MF, Kuhl A, Jennrich S, Watzlawick R, Hoffmann U, Wolff T, Norley S, Scheffold A, Stumhofer JS, Saris CJ, Schwab JM, Hunter CA, Debes GF, and Hamann A. 2014. Timed action of IL-27 protects from immunopathology while preserving defense in influenza. PLoS Pathog 10: e1004110. [PubMed: 24809349]
37. Zeng R, Zhang H, Hai Y, Cui Y, Wei L, Li N, Liu J, Li C, and Liu Y. 2012. Interleukin-27 inhibits vaccine-enhanced pulmonary disease following respiratory syncytial virus infection by regulating cellular memory responses. J Virol 86: 4505–4517. [PubMed: 22301139]
38. Liu L, Cao Z, Chen J, Li R, Cao Y, Zhu C, Wu K, Wu J, Liu F, and Zhu Y. 2012. Influenza A virus induces interleukin-27 through cyclooxygenase-2 and protein kinase A signaling. J Biol Chem 287: 11899–11910. [PubMed: 22343630]
39. Imamichi T, Yang J, Huang DW, Brann TW, Fullmer BA, Adelsberger JW, Lempicki RA, Baseler MW, and Lane HC. 2008. IL-27, a novel anti-HIV cytokine, activates multiple interferon-inducible genes in macrophages. AIDS 22: 39–45. [PubMed: 18090390]
40. Xia L, Tan T, Li Y, Zhong Q, and Shi M. 2019. Blockade of IL-27 signaling ameliorates herpes stromal keratitis with upregulated CD4(+) Foxp3(+) regulatory T cells influx in mice. Indian J Ophthalmol 67: 1821–1828. [PubMed: 31638041]

41. Pirhonen J, Siren J, Julkunen I, and Matikainen S. 2007. IFN-alpha regulates Toll-like receptor-mediated IL-27 gene expression in human macrophages. J Leukocyte Biol 82: 1185–1192. [PubMed: 17684041]
42. Hunter CA, and Kastelein R. 2012. Interleukin-27: balancing protective and pathological immunity. Immunity 37: 960–969. [PubMed: 23244718]
43. Liu J, Guan X, and Ma X. 2007. Regulation of IL-27 p28 gene expression in macrophages through MyD88- and interferon-gamma-mediated pathways. J Exp Med 204: 141–152. [PubMed: 17227910]
44. Yoshida H, and Hunter CA. 2015. The immunobiology of interleukin-27. Annu Rev Immunol 33: 417–443. [PubMed: 25861977]
45. Yoshida H, Hamano S, Senaldi G, Covey T, Faggioni R, Mu S, Xia M, Wakeham AC, Nishina H, Potter J, Saris CJ, and Mak TW. 2001. WSX-1 is required for the initiation of Th1 responses and resistance to L. major infection. Immunity 15: 569–578. [PubMed: 11672539]
46. Chen Q, Ghilardi N, Wang H, Baker T, Xie MH, Gurney A, Grewal IS, and de Sauvage FJ. 2000. Development of Th1-type immune responses requires the type I cytokine receptor TCCR. Nature 407: 916–920. [PubMed: 11057672]
47. Mascanfroni ID, Yeste A, Vieira SM, Burns EJ, Patel B, Sloma I, Wu Y, Mayo L, Ben-Hamo R, Efroni S, Kuchroo VK, Robson SC, and Quintana FJ. 2013. IL-27 acts on DCs to suppress the T cell response and autoimmunity by inducing expression of the immunoregulatory molecule CD39. Nat Immunol 14: 1054–1063. [PubMed: 23995234]
48. Treat BR, Bidula SM, St Leger AJ, Hendricks RL, and Kinchington PR. 2020. Herpes Simplex Virus 1-Specific CD8(+) T Cell Priming and Latent Ganglionic Retention Are Shaped by Viral Epitope Promoter Kinetics. J Virol 94.
49. Assouvie A, Daley-Bauer LP, and Rousselet G. 2018. Growing Murine Bone Marrow-Derived Macrophages. Methods Mol Biol 1784: 29–33. [PubMed: 29761385]
50. Wang W, Li J, Wu K, Azhati B, and Rexiati M. 2016. Culture and Identification of Mouse Bone Marrow-Derived Dendritic Cells and Their Capability to Induce T Lymphocyte Proliferation. Med Sci Monit 22: 244–250. [PubMed: 26802068]
51. Banerjee K, Biswas PS, Kim B, Lee S, and Rouse BT. 2004. CXCR2−/− mice show enhanced susceptibility to herpetic stromal keratitis: a role for IL-6-induced neovascularization. J Immunol 172: 1237–1245. [PubMed: 14707102]
52. Gaddipati S, Estrada K, Rao P, Jerome AD, and Suvas S. 2015. IL-2/anti-IL-2 antibody complex treatment inhibits the development but not the progression of herpetic stromal keratitis. J Immunol 194: 273–282. [PubMed: 25411200]
53. Kwock JT, Handfield C, Suwanpradid J, Hoang P, McFadden MJ, Labagnara KF, Floyd L, Shannon J, Uppala R, Sarkar MK, Gudjonsson JE, Corcoran DL, Lazear HM, Sempowski G, Horner SM, and MacLeod AS. 2020. IL-27 signaling activates skin cells to induce innate antiviral proteins and protects against Zika virus infection. Sci Adv 6: eaay3245. [PubMed: 32270034]
54. de Aquino MT, Kapil P, Hinton DR, Phares TW, Puntambekar SS, Savarin C, Bergmann CC, and Stohlman SA. 2014. IL-27 limits central nervous system viral clearance by promoting IL-10 and enhances demyelination. J Immunol 193: 285–294. [PubMed: 24890725]
55. Amsden H, Kourko O, Roth M, and Gee K. 2022. Antiviral Activities of Interleukin-27: A Partner for Interferons? Front Immunol 13: 902853. [PubMed: 35634328]
56. Hori J 2008. Mechanisms of immune privilege in the anterior segment of the eye: what we learn from corneal transplantation. J Ocul Biol Dis Infor 1: 94–100. [PubMed: 20072639]
57. Cursiefen C 2007. Immune privilege and angiogenic privilege of the cornea. Chem Immunol Allergy 92: 50–57. [PubMed: 17264482]
58. Yun H, Yee MB, Lathrop KL, Kinchington PR, Hendricks RL, and St Leger AJ. 2020. Production of the Cytokine VEGF-A by CD4(+) T and Myeloid Cells Disrupts the Corneal Nerve Landscape and Promotes Herpes Stromal Keratitis. Immunity 53: 1050–1062 e1055. [PubMed: 33207210]
59. Suryawanshi A, Mulik S, Sharma S, Reddy PB, Sehrawat S, and Rouse BT. 2011. Ocular neovascularization caused by herpes simplex virus type 1 infection results from breakdown of binding between vascular endothelial growth factor A and its soluble receptor. J Immunol 186: 3653–3665. [PubMed: 21325621]

60. Pflanz S, Timans JC, Cheung J, Rosales R, Kanzler H, Gilbert J, Hibbert L, Churakova T, Travis M, Vaisberg E, Blumenschein WM, Mattson JD, Wagner JL, To W, Zurawski S, McClanahan TK, Gorman DM, Bazan JF, de Waal Malefyt R, Rennick D, and Kastelein RA. 2002. IL-27, a heterodimeric cytokine composed of EBI3 and p28 protein, induces proliferation of naive CD4+ T cells. Immunity 16: 779–790. [PubMed: 12121660]

61. Banchereau J, Briere F, Caux C, Davoust J, Lebecque S, Liu YJ, Pulendran B, and Palucka K. 2000. Immunobiology of dendritic cells. Annu Rev Immunol 18: 767–811. [PubMed: 10837075]

62. Buela KA, and Hendricks RL. 2015. Cornea-infiltrating and lymph node dendritic cells contribute to CD4+ T cell expansion after herpes simplex virus-1 ocular infection. J Immunol 194: 379–387. [PubMed: 25422507]

63. Guerriero JL 2019. Macrophages: Their Untold Story in T Cell Activation and Function. Int Rev Cell Mol Biol 342: 73–93. [PubMed: 30635094]

64. Peng X, Kasran A, Warmerdam PA, de Boer M, and Ceuppens JL. 1996. Accessory signaling by CD40 for T cell activation: induction of Th1 and Th2 cytokines and synergy with interleukin-12 for interferon-gamma production. Eur J Immunol 26: 1621–1627. [PubMed: 8766570]

65. Ma DY, and Clark EA. 2009. The role of CD40 and CD154/CD40L in dendritic cells. Semin Immunol 21: 265–272. [PubMed: 19524453]

66. Macatonia SE, Hsieh CS, Murphy KM, and O'Garra A. 1993. Dendritic cells and macrophages are required for Th1 development of CD4+ T cells from alpha beta TCR transgenic mice: IL-12 substitution for macrophages to stimulate IFN-gamma production is IFN-gamma-dependent. Int Immunol 5: 1119–1128. [PubMed: 7902129]

67. Jung JY, Roberts LL, and Robinson CM. 2015. The presence of interleukin-27 during monocyte-derived dendritic cell differentiation promotes improved antigen processing and stimulation of T cells. Immunology 144: 649–660. [PubMed: 25346485]

68. Hamrah P, Huq SO, Liu Y, Zhang Q, and Dana MR. 2003. Corneal immunity is mediated by heterogeneous population of antigen-presenting cells. J Leukoc Biol 74: 172–178. [PubMed: 12885933]

69. Kuffova L, Netukova M, Duncan L, Porter A, Stockinger B, and Forrester JV. 2008. Cross presentation of antigen on MHC class II via the draining lymph node after corneal transplantation in mice. J Immunol 180: 1353–1361. [PubMed: 18209029]

70. Cella M, Engering A, Pinet V, Pieters J, and Lanzavecchia A. 1997. Inflammatory stimuli induce accumulation of MHC class II complexes on dendritic cells. Nature 388: 782–787. [PubMed: 9285591]

71. Shukla SD, and Valyi-Nagy T. 2022. Host Molecules That Promote Pathophysiology of Ocular Herpes. Front Microbiol 13: 818658. [PubMed: 35145504]

72. Cao Y, Zhang R, Zhang W, Zhu C, Yu Y, Song Y, Wang Q, Bai L, Liu Y, Wu K, and Wu J. 2014. IL-27, a cytokine, and IFN-lambda1, a type III IFN, are coordinated to regulate virus replication through type I IFN. J Immunol 192: 691–703. [PubMed: 24337382]

73. Sweeney CM, Lonergan R, Basdeo SA, Kinsella K, Dungan LS, Higgins SC, Kelly PJ, Costelloe L, Tubridy N, Mills KH, and Fletcher JM. 2011. IL-27 mediates the response to IFN-beta therapy in multiple sclerosis patients by inhibiting Th17 cells. Brain Behav Immun 25: 1170–1181. [PubMed: 21420486]

74. Cheng J, Myers TG, Levinger C, Kumar P, Kumar J, Goshu BA, Bosque A, and Catalfamo M. 2022. IL-27 induces IFN/STAT1-dependent genes and enhances function of TIGIT(+) HIVGag-specific T cells. iScience 25: 103588. [PubMed: 35005538]

75. Lenschow DJ, Lai C, Frias-Staheli N, Giannakopoulos NV, Lutz A, Wolff T, Osiak A, Levine B, Schmidt RE, Garcia-Sastre A, Leib DA, Pekosz A, Knobeloch KP, Horak I, and Virgin H. W. t.. 2007. IFN-stimulated gene 15 functions as a critical antiviral molecule against influenza, herpes, and Sindbis viruses. Proc Natl Acad Sci U S A 104: 1371–1376. [PubMed: 17227866]

76. Zhang M, Zhang MX, Zhang Q, Zhu GF, Yuan L, Zhang DE, Zhu Q, Yao J, Shu HB, and Zhong B. 2016. USP18 recruits USP20 to promote innate antiviral response through deubiquitinating STING/MITA. Cell Res 26: 1302–1319. [PubMed: 27801882]

77. Lobo AM, Agelidis AM, and Shukla D. 2019. Pathogenesis of herpes simplex keratitis: The host cell response and ocular surface sequelae to infection and inflammation. Ocul Surf 17: 40–49. [PubMed: 30317007]

78. Hunter CA 2005. New IL-12-family members: IL-23 and IL-27, cytokines with divergent functions. Nat Rev Immunol 5: 521–531. [PubMed: 15999093]

79. Pirhonen J, Siren J, Julkunen I, and Matikainen S. 2007. IFN-alpha regulates Toll-like receptor-mediated IL-27 gene expression in human macrophages. J Leukoc Biol 82: 1185–1192. [PubMed: 17684041]

80. Dai L, Lidie KB, Chen Q, Adelsberger JW, Zheng X, Huang D, Yang J, Lempicki RA, Rehman T, Dewar RL, Wang Y, Hornung RL, Canizales KA, Lockett SJ, Lane HC, and Imamichi T. 2013. IL-27 inhibits HIV-1 infection in human macrophages by down-regulating host factor SPTBN1 during monocyte to macrophage differentiation. J Exp Med 210: 517–534. [PubMed: 23460728]

81. Li SF, Gong MJ, Zhao FR, Shao JJ, Xie YL, Zhang YG, and Chang HY. 2018. Type I Interferons: Distinct Biological Activities and Current Applications for Viral Infection. Cell Physiol Biochem 51: 2377–2396. [PubMed: 30537741]

82. Kumaran Satyanarayanan S, El Kebir D, Soboh S, Butenko S, Sekheri M, Saadi J, Peled N, Assi S, Othman A, Schif-Zuck S, Feuermann Y, Barkan D, Sher N, Filep JG, and Ariel A. 2019. IFN-beta is a macrophage-derived effector cytokine facilitating the resolution of bacterial inflammation. Nat Commun 10: 3471. [PubMed: 31375662]

83. Tan G, Xiao Q, Song H, Ma F, Xu F, Peng D, Li N, Wang X, Niu J, Gao P, Qin FX, and Cheng G. 2018. Type I IFN augments IL-27-dependent TRIM25 expression to inhibit HBV replication. Cell Mol Immunol 15: 272–281. [PubMed: 28194021]

84. Danastas K, Miranda-Saksena M, and Cunningham AL. 2020. Herpes Simplex Virus Type 1 Interactions with the Interferon System. Int J Mol Sci 21.

85. Christensen MH, Jensen SB, Miettinen JJ, Luecke S, Prabakaran T, Reinert LS, Mettenleiter T, Chen ZJ, Knipe DM, Sandri-Goldin RM, Enquist LW, Hartmann R, Mogensen TH, Rice SA, Nyman TA, Matikainen S, and Paludan SR. 2016. HSV-1 ICP27 targets the TBK1-activated STING signalsome to inhibit virus-induced type I IFN expression. EMBO J 35: 1385–1399. [PubMed: 27234299]

86. Xing J, Ni L, Wang S, Wang K, Lin R, and Zheng C. 2013. Herpes simplex virus 1-encoded tegument protein VP16 abrogates the production of beta interferon (IFN) by inhibiting NF-kappaB activation and blocking IFN regulatory factor 3 to recruit its coactivator CBP. J Virol 87: 9788–9801. [PubMed: 23824799]

87. Owaki T, Asakawa M, Morishima N, Hata K, Fukai F, Matsui M, Mizuguchi J, and Yoshimoto T. 2005. A role for IL-27 in early regulation of Th1 differentiation. J Immunol 175: 2191–2200. [PubMed: 16081786]

88. Montes de Oca M, de Labastida Rivera F, Winterford C, Frame TCM, Ng SS, Amante FH, Edwards CL, Bukali L, Wang Y, Uzonna JE, Kuns RD, Zhang P, Kabat A, Klein Geltink RI, Pearce EJ, Hill GR, and Engwerda CR. 2020. IL-27 signalling regulates glycolysis in Th1 cells to limit immunopathology during infection. PLoS Pathog 16: e1008994. [PubMed: 33049000]

89. Iwasaki Y, Fujio K, Okamura T, and Yamamoto K. 2015. Interleukin-27 in T cell immunity. Int J Mol Sci 16: 2851–2863. [PubMed: 25633106]

90. Ivashkiv LB, and Donlin LT. 2014. Regulation of type I interferon responses. Nat Rev Immunol 14: 36–49. [PubMed: 24362405]

91. Mesev EV, LeDesma RA, and Ploss A. 2019. Decoding type I and III interferon signalling during viral infection. Nat Microbiol 4: 914–924. [PubMed: 30936491]

92. Strickland AB, Sun D, Sun P, Chen Y, Liu G, and Shi M. 2022. IL-27 Signaling Promotes Th1 Responses and Is Required to Inhibit Fungal Growth in the Lung during Repeated Exposure to Aspergillus fumigatus. Immunohorizons 6: 78–89. [PubMed: 35064029]

93. Wang H, Meng R, Li Z, Yang B, Liu Y, Huang F, Zhang J, Chen H, and Wu C. 2011. IL-27 induces the differentiation of Tr1-like cells from human naive CD4+ T cells via the phosphorylation of STAT1 and STAT3. Immunol Lett 136: 21–28. [PubMed: 21115047]

94. Visperas A, Do JS, Bulek K, Li X, and Min B. 2014. IL-27, targeting antigen-presenting cells, promotes Th17 differentiation and colitis in mice. Mucosal Immunol 7: 625–633. [PubMed: 24129161]

Key points:

- IL-27 limits HSV-1 shedding from the cornea and suppresses HSK progression.
- IL-27 modulates APC-mediated HSV-1 antigen presentation to regulate Th1 responses.
- IL-27 promotes macrophage survival and IFN-β responses after HSV-1 infection.

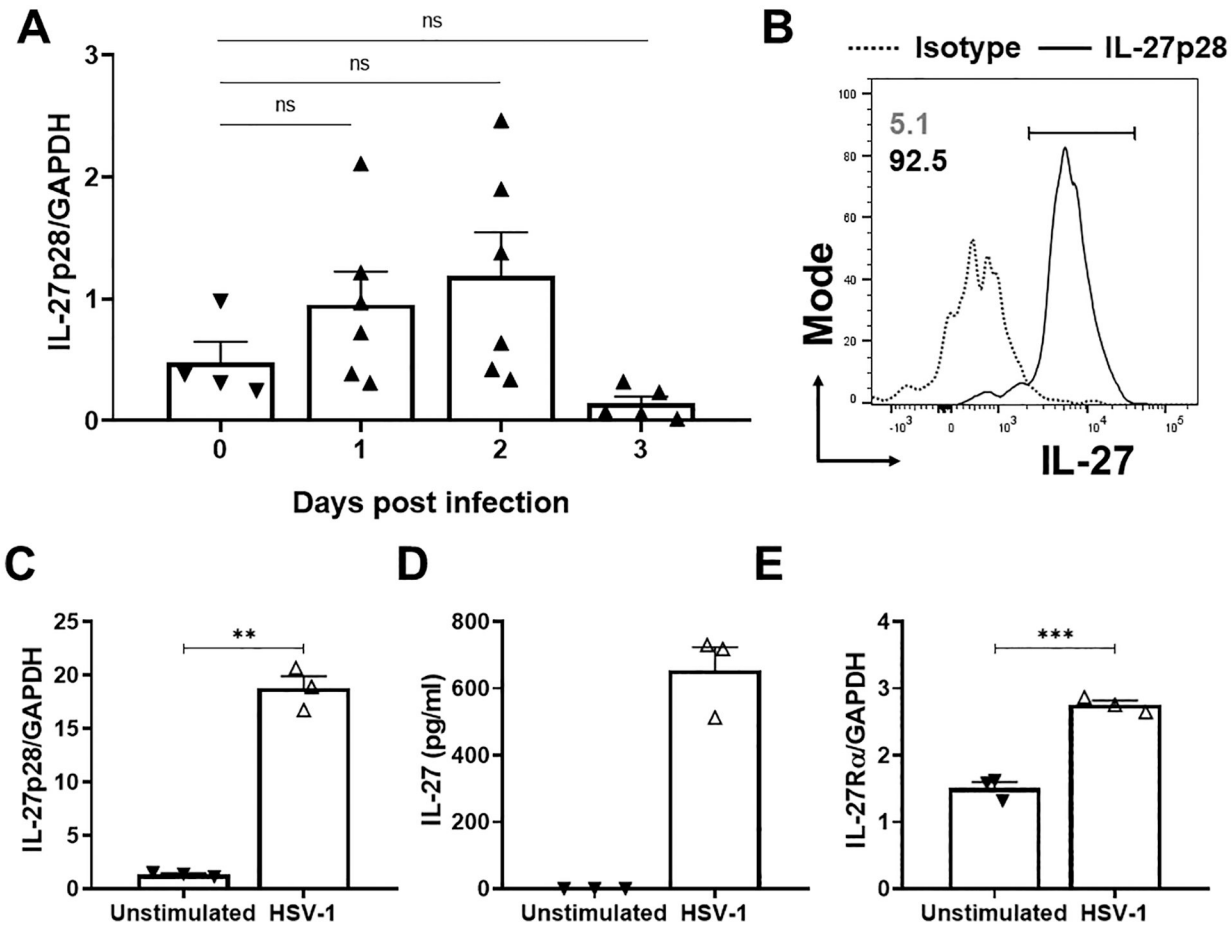

Figure 1. HSV-1 infection induces IL-27 responses.

(A) qPCR analysis showing the expression of IL-27 levels in the corneas of WT mice infected with 10^4 PFU of HSV-1. 2–3 corneas were pooled to make one replicate for analysis at each time point. **(B)** Histograms showing IL-27 producing corneal macrophages ($CD11b^+F4/80^+$) on day 2 pi. **(C)** qPCR analysis examining IL-27 mRNA expression levels in BMDM stimulated with HSV-1 for 24 hours. **(D)** IL-27 concentration was measured in BMDM culture supernatant stimulated with HSV-1 for 24 hours. **(E)** IL-27Rα expression levels in BMDM cells stimulated with HSV-1 for 24 hours. Fold change was normalized to GAPDH. The data shown is one representative experiment out of two independent experiments. Statistical significance was calculated by one way ANOVA with Dunnet's test to compare multiple groups and the parametric unpaired Student's t-test for comparing two groups. **p<0.01; ***p< 0.001; ns, non-significant. Error bars show mean ± SEM.

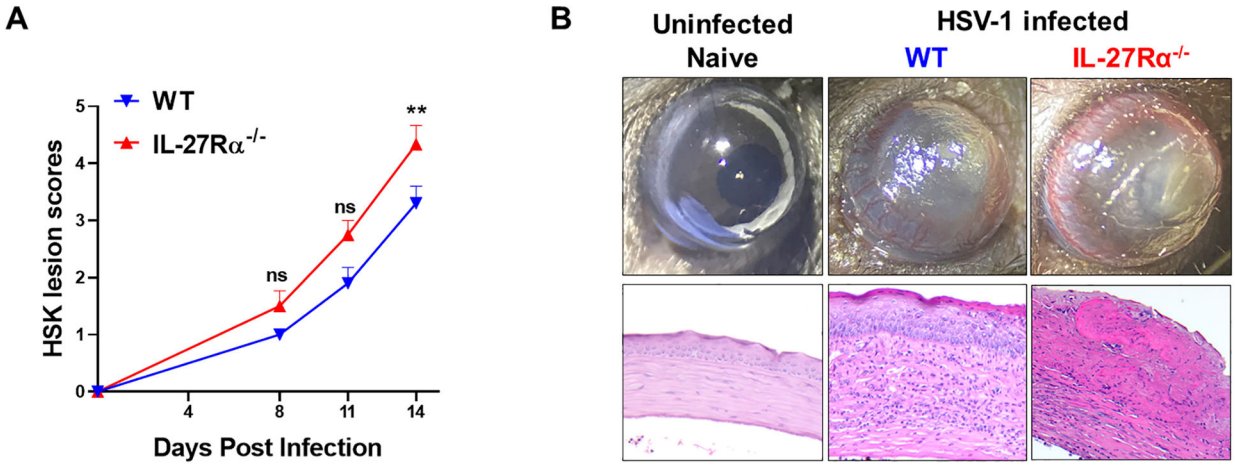

Figure 2. IL-27 suppresses HSK disease severity.

(A) The kinetic progression of HSK lesions in WT and IL-27Rα$^{-/-}$ mice infected with 10^4 PFU of HSV-1. Eyes with a score of zero at day 15 pi were considered uninfected and excluded from both groups of infected mice. **(B)** Representative eye images (top panel) showing naïve uninfected (left) and the HSK severity on day 14 pi of WT (middle), and IL-27Rα$^{-/-}$ (right) mice and representative H&E stained corneal sections (bottom panel) collected on day 15 pi. H&E stained corneal sections were taken at a magnification of 200X. Data represent one independent experiment out of four experiments carried out with 4–5 mice in each group. Statistical significance was calculated using the non-parametric unpaired Mann–Whitney U test. **p<0.01; ***p< 0.001; ns, non-significant. Error bars show mean ± SEM.

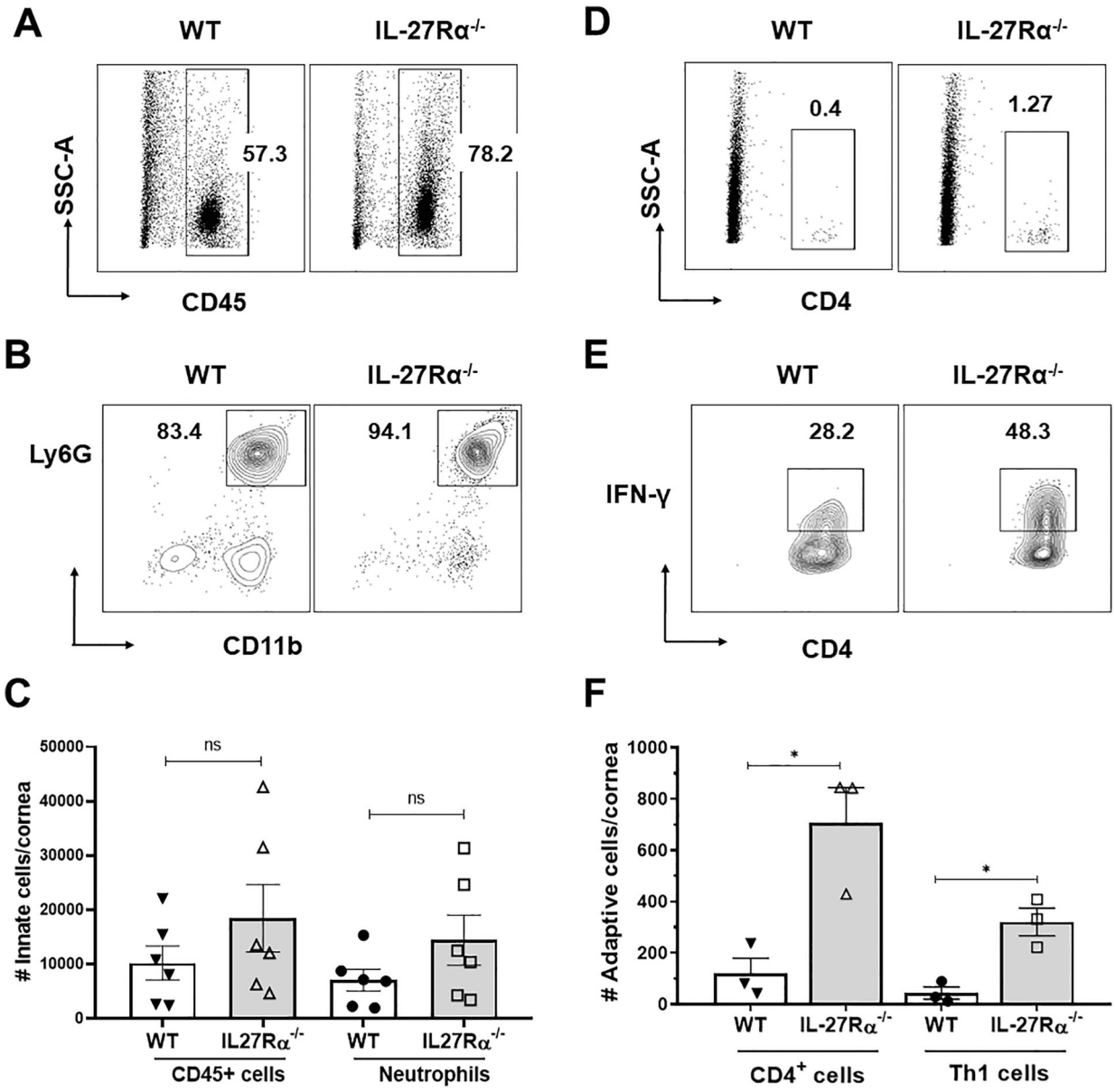

Figure 3. IL-27 modulates infiltration of inflammatory immune responses in HSV-1 infected cornea.

(A) Representative FACS plots showing total leukocytes ($CD45^+$) in cornea collected from WT and IL-27Rα$^{-/-}$ mice on day 15 pi. **(B)** Representative FACS plots of neutrophils ($CD45^+CD11b^+F4/80^-Ly6G^+$). **(C)** Graph showing the total number of leukocytes and neutrophils per cornea of WT and IL-27Rα$^{-/-}$ mice on day 15 pi. Data shown represents a summary of four experiments. **(D)** Representative FACS plots showing $CD4^+$ T cells in the cornea of WT and IL-27Rα$^{-/-}$ mice on day 15 pi. **(G)** Representative FACS plot of Th1 cells (after stimulation with PMA/Ionomycin for 5 hours) in WT and IL-27Rα$^{-/-}$ corneas on day 15 pi. **(F)** Bar graph showing the number of $CD4^+$ T cells and Th1 cells per cornea. Data shown is one representative experiment out of four independent experiments carried out with 4–5 mice in each group. 3–4 corneas were pooled to make one replicate for all

flow cytometric analyses. Statistical significance was calculated by the parametric unpaired Student's t-test. *$p < 0.05$; ns, non-significant. Error bars show mean ± SEM.

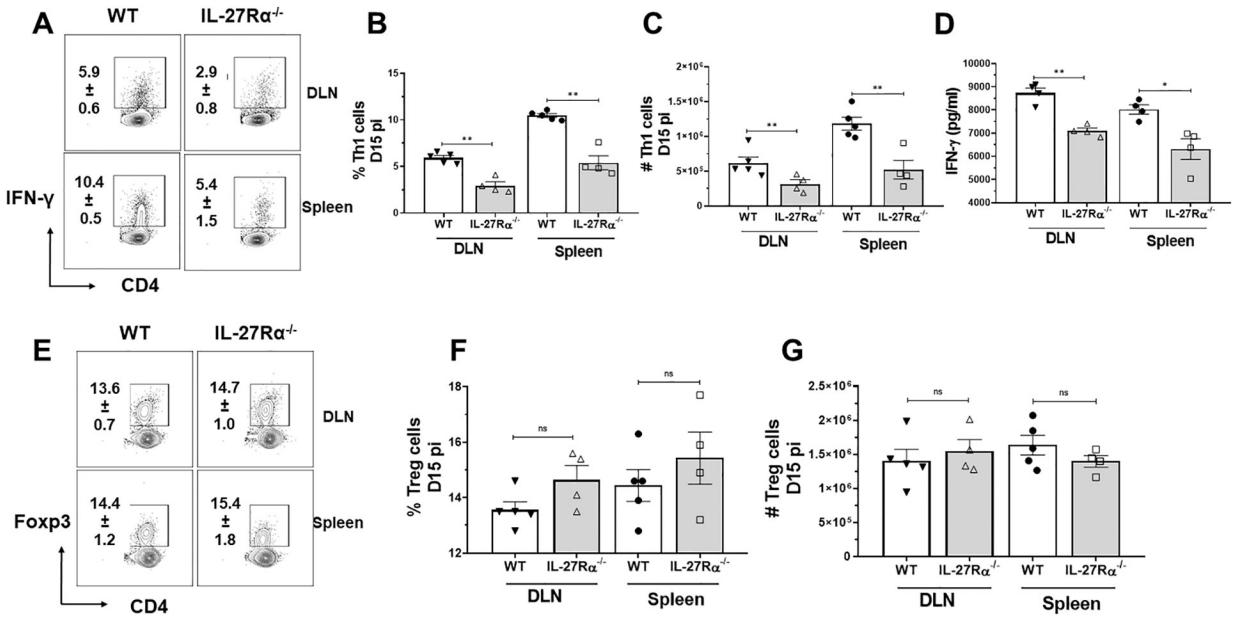

Figure 4. IL-27 regulates Th1 differentiation in secondary lymphoid organs.

(A) Representative FACS plot showing Th1 cells (after stimulation with PMA/Ionomycin for 5 hours) in DLN and spleen of WT and IL-27Rα$^{-/-}$ mice infected with 10^4 PFU of HSV-1 on day 15 pi. Bar graphs showing the **(B)** frequencies and **(C)** the number of Th1 (CD4$^+$IFN-γ$^+$) cells in DLN and spleen of WT and IL-27Rα$^{-/-}$ mice on day 15 pi. **(D)** IFN-γ levels in the culture supernatant of DLN and spleen cells (stimulated with UV-inactivated HSV-1 for 24 hours) isolated from HSV-1 infected WT and IL-27Rα$^{-/-}$ mice on day 15 pi. **(E)** Representative FACS plots showing Treg (CD4$^+$Foxp3$^+$) cells in DLN and spleen of WT and IL-27Rα$^{-/-}$ mice on day 15 pi. Bar graphs showing the **(F)** frequencies and **(G)** the number of Treg cells in DLN and spleen of WT and IL-27Rα$^{-/-}$ mice on day 15 pi. Data shown is one representative experiment out of the four independent experiments carried out with 4–5 mice in each group. Statistical levels of significance were analyzed by parametric unpaired Student's t-test. *p< 0.05; **p<0.01; ns, non-significant. Error bars show mean ± SEM.

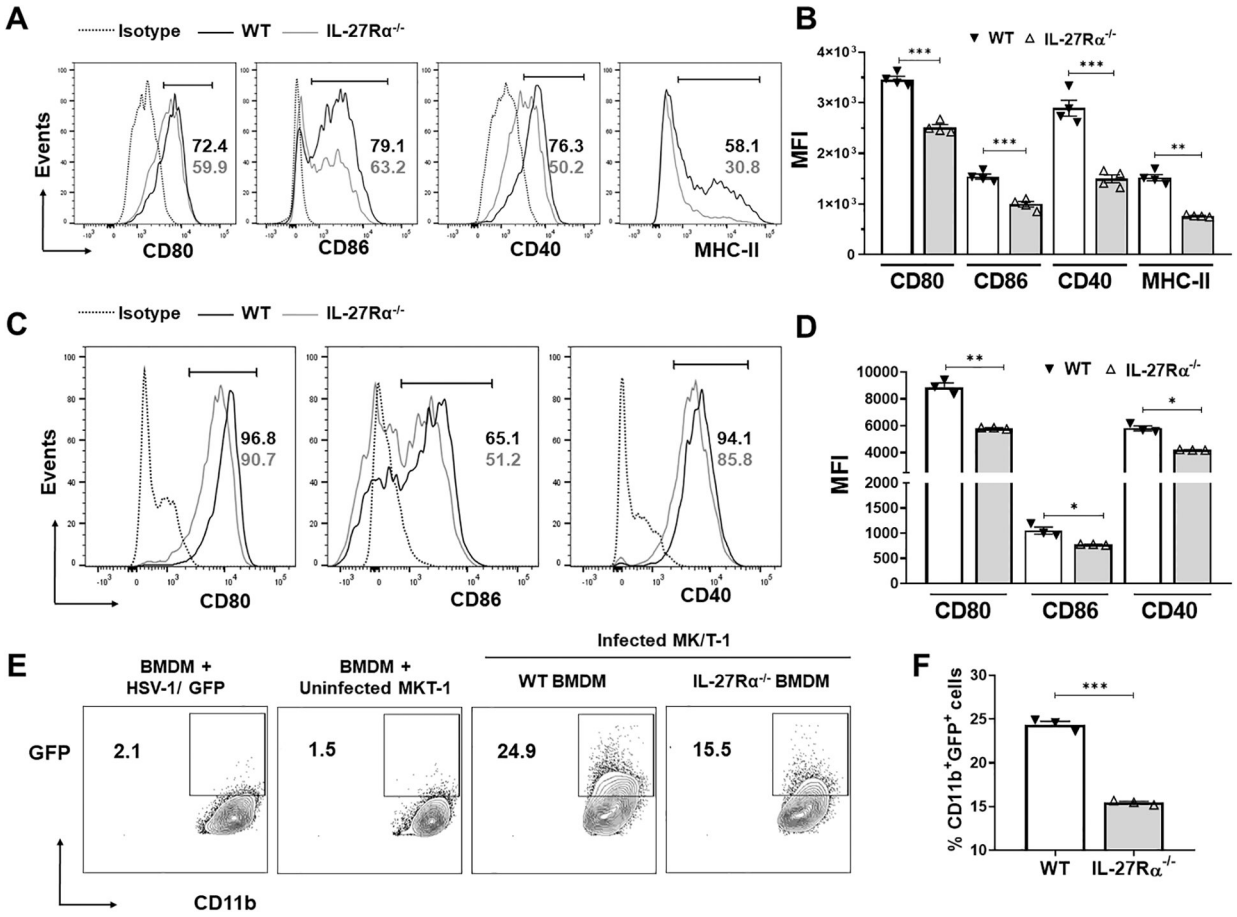

Figure 5. IL-27 is critical for maturation and efficient antigen uptake by APCs after HSV-1 infection.

(A) Histogram overlay and **(B)** bar graphs showing mean fluorescence intensity (MFI) of CD80, CD86, CD40 and MHC-II expression from WT and IL-27Rα$^{-/-}$ BMDCs, stimulated with 2 MOI of HSV-1 for 24 hours. **(C)** Histogram overlay and **(D)** bar graphs showing MFI of CD80, CD86, and CD40 expression from WT and IL-27Rα$^{-/-}$ BMDMs, stimulated with 2 MOI of HSV-1 for 24 hours. **(E)** Representative FACs plot showing phagocytosis of HSV-1/GFP infected MKT-1 cells by WT and IL-27Rα$^{-/-}$ BMDMs. HSV-1/GFP directly infected with BMDM and uninfected MKT-1 cells co-cultured with BMDM were used as additional controls. **(F)** Graph showing the frequency of phagocytic (CD11b^{+}GFP^{+}) BMDMs cultured from WT and IL-27Rα$^{-/-}$ mice. The data shown represents one experiment out of two independent experiments. Statistical significance were analyzed by parametric unpaired Student's t-test.*p< 0.05; **p<0.01; ***p<0.001. Error bars show mean ± SEM.

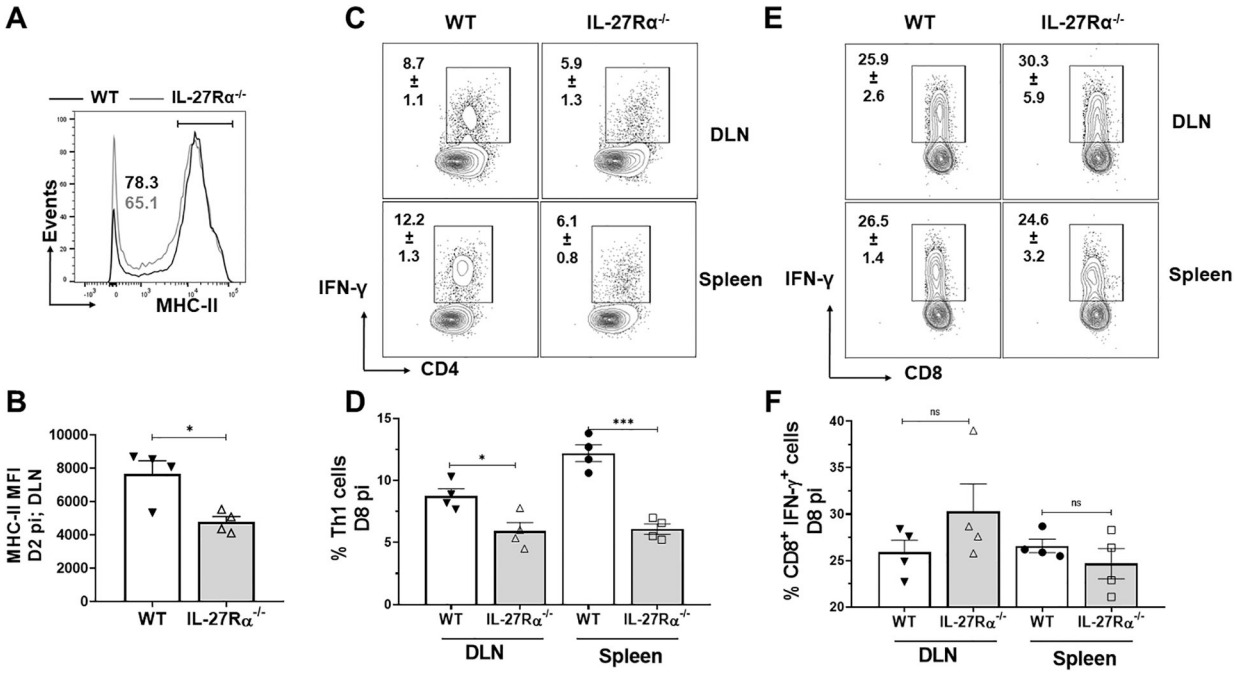

Figure 6. IL-27 regulates APC maturation and Th1 differentiation in secondary lymphoid organs.

(A) Histogram overlay and **(B)** bar graphs showing MFI of MHC-II expression in $CD11c^+$ cells in DLNs of WT and IL-27R$\alpha^{-/-}$ mice on day 2 pi. **(C)** Representative FACS plot showing Th1 cells (after stimulation with PMA/Ionomycin for 5 hours) in DLN and spleen of WT and IL-27R$\alpha^{-/-}$ mice on day 8 pi. **(D)** Bar graphs showing the frequencies of Th1 ($CD4^+$ IFN-γ^+) cells in DLN and spleen of WT and IL-27R$\alpha^{-/-}$ mice on day 8 pi. **(E)** Representative FACS plot showing effector $CD8^+$IFN-γ^+ T cells (after stimulation with PMA/Ionomycin for 5 hours) in DLN and spleen of WT and IL-27R$\alpha^{-/-}$ mice on day 8 pi. **(F)** Bar graphs showing the frequencies of $CD8^+$IFN-γ^+ cells in DLN and spleen of WT and IL-27R$\alpha^{-/-}$ mice on day 8 pi. Data shown represents one experiment out of the three independent experiments carried out with 4–5 mice in each group. Statistical significance were analyzed by parametric unpaired Student's t-test. *p< 0.05; ***p<0.001; ns, non-significant. Error bars show mean ± SEM.

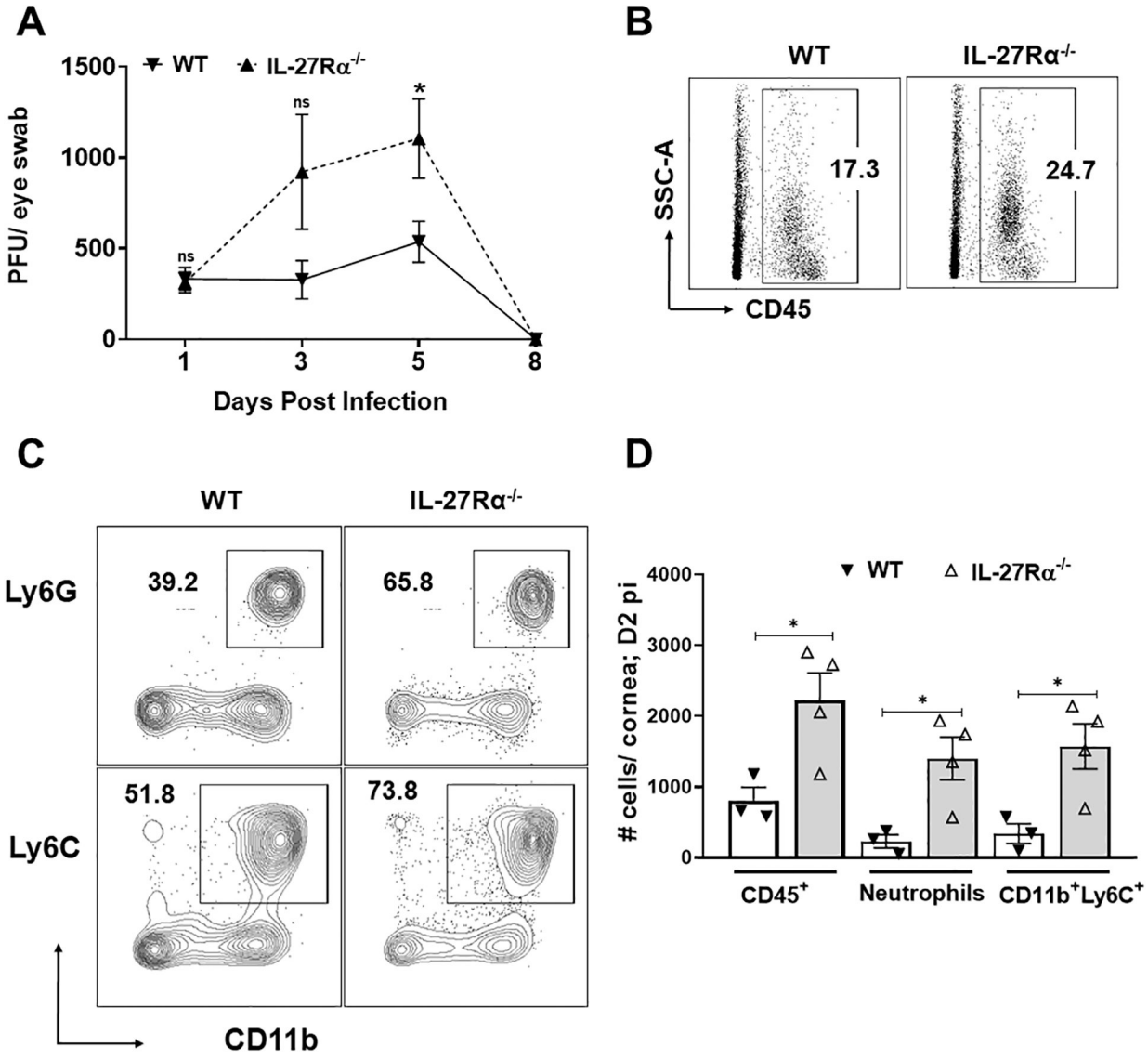

Figure 7. IL-27 suppresses HSV-1 replication and regulates early inflammatory response in the cornea.

(A) HSV-1 titers were measured by plaque assay in eye swabs collected from WT and IL-27Rα$^{-/-}$ mice on days 1, 2, and 3 after HSV-1 infection. Eye swabs with a viral titer of zero were considered uninfected and excluded. n=16 (WT) and n= 18 (IL-27Rα$^{-/-}$). The data represents two independent experiments. Representative FACS plots of **(B)** total leukocytes (CD45^{+}), **(C)** neutrophils (CD45^{+}CD11b^{+}F4/80^{-}Ly6G^{+}) and inflammatory monocytes (CD45^{+}CD11b^{+}Ly6C^{+}) in WT and IL-27Rα$^{-/-}$ cornea on day 2 pi. **(D)** Bar graph showing the number of total leukocytes, neutrophils and inflammatory monocytes per cornea of WT and IL-27Rα$^{-/-}$ mice on day 2 pi. 3–4 corneas were pooled to make one replicate for all flow cytometric analyses. The data shown represents one experiment out of two independent experiments. Statistical significance was calculated by the parametric unpaired Student's t-test. *p< 0.05; ns, non-significant. Error bars show mean ± SEM.

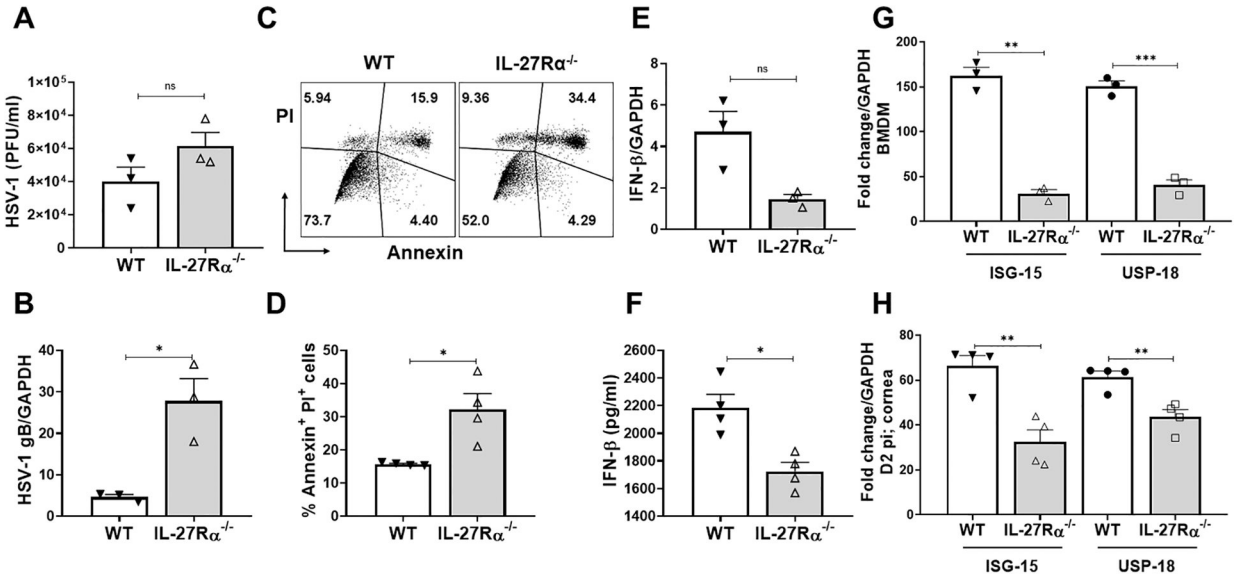

Figure 8. IL-27 is critical for the induction of macrophage-intrinsic anti-viral responses and macrophage survival during HSV-1 infection.

(A) HSV-1 titers in media collected from WT and IL-27Rα$^{-/-}$ BMDM infected with 2 MOI of HSV-1 for 24 hours were quantified by plaque assay. **(B)** qPCR analysis showing relative expression of HSV-1 gB in WT and IL-27Rα$^{-/-}$ BMDM after 24 hours of HSV-1 infection. **(C)** Representative FACS plots and **(D)** frequencies of late apoptotic (Annexin^{+} PI^{+}) cells in WT and IL-27Rα$^{-/-}$ BMDM after 24 hours of HSV-1 infection. **(E)** qPCR analysis showing the relative expression of IFN-β in WT and IL-27Rα$^{-/-}$ BMDM after 24 hours of HSV-1 infection. **(F)** IFN-β production in WT and IL-27Rα$^{-/-}$ BMDM after 24 hours of HSV-1 infection by ELISA. **(G)** qPCR analysis showing the relative expression of ISG-15 and USP-18 in WT and IL-27Rα$^{-/-}$ BMDM after 24 hours of HSV-1 infection. **(H)** qPCR analysis showing the relative expression of ISG-15 and USP-18 in WT and IL-27Rα$^{-/-}$ corneas on day 2 pi. The data shown represents one experiment out of two independent experiments. Statistical significance was calculated by the parametric unpaired Student's t-test. *p< 0.05 **p<0.01 ***p<0.001; ns, non-significant. Error bars show mean ± SEM.